Received: 11 August 2017 | Revised: 2 February 2018 | Accepted: 6 February 2018

DOI: 10.1002/ajpa.23446

RESEARCH ARTICLE

WILEY American Journal of PHYSICAL ANTHROPOLOGY

Locomotor activity, growth hormones, and systemic robusticity: An investigation of cranial vault thickness in mouse lines bred for high endurance running

L. E. Copes[1] | H. Schutz[2] | E. M. Dlugosz[3] | S. Judex[4] | T. Garland Jr[3]

[1]Department of Medical Sciences, Frank H. Netter MD School of Medicine, Quinnipiac University, Hamden, Connecticut 06518

[2]Department of Biology, Pacific Lutheran University, Tacoma, Washington, DC 98447

[3]Department of Biology, University of California, Riverside, Riverside, California 92521

[4]Department of Biomedical Engineering, Stony Brook University, Stony Brook, New York 11794

Correspondence
L. E. Copes, Department of Medical Sciences, Frank H. Netter MD School of Medicine, Quinnipiac University, Hamden, Connecticut 06518.
Email: lynn.copes@quinnipiac.edu

Funding information
NSF, Grant Numbers: DDIG 0925793, IOB-0543429, DEB-1655362; Wenner-Gren Dissertation Grant, Grant Number: 8102

Abstract

Objectives: To use a mouse model to investigate the relationships among the components of the systemic robusticity hypothesis (SRH): voluntary exercise on wheels, spontaneous physical activity (SPA) in cages, growth hormones, and skeletal robusticity, especially cranial vault thickness (CVT).

Materials and Methods: Fifty female mice from lines artificially selected for high running (HR) and 50 from nonselected control (C) lines were housed in cages with (Active) or without wheels (Sedentary). Wheel running and SPA were monitored daily. The experiment began at 24–27 days of age and lasted 12 weeks. Food consumption was measured weekly. Mice were skeletonized and their interparietal, parietal, humerus, and femur were μCT scanned. Mean total thickness of the parietal and interparietal bones was determined, along with thickness of the cortical and diploe layers individually. Geometric cross-sectional indicators of strength were calculated for the long bones. Blood samples were assayed for IGF-1 and IGFBP-3.

Results: Physical activity differed significantly among groups, based both on linetype (C vs. HR) and activity (A vs. S). However, contrary to our predictions, the ratio of IGF-1 to IGFBP-3 was higher in C mice than in HR mice. Neither CVT nor postcranial robusticity was affected by linetype or activity, nor were most measures of CVT and postcranial robusticity significantly associated with one another.

Discussion: Our results fail to provide support for the systemic robusticity hypothesis, suggesting it is important to rethink the long-standing theory that increased CVT in *Homo erectus* reflects increased physical activity compared other hominin species.

KEYWORDS
artificial selection, cranial vault thickness, growth hormones, locomotor activity, *Mus musculus*

1 | INTRODUCTION

Cranial vault thickness (CVT) has been measured and reported repeatedly by anthropologists studying modern human populations, especially when it is unusually thick or thin (Baab, Freidline, Wang, & Hanson, 2010; Bernal, Perez, & Gonzalez, 2006; Brown, 1992; Brown, 1994; Curnoe, 2009; Hrdlicka, 1910; Lahr & Wright, 1996). However, it is the extremely thick cranial vaults noted as a diagnostic characteristic of *Homo erectus* since the first fossil of the species was identified (Andrews, 1984; Antón, 2002; Antón, 2003; Bilsborough & Wood, 1988; Dubois, 1937; Weidenreich, 1943) that capture the interest of many researchers. However, the mechanisms underlying this increase in CVT have not been thoroughly investigated.

During the past two decades, the most widely cited explanation for increased CVT in *Homo erectus* is Lieberman's Systemic Robusticity Hypothesis (Lieberman, 1996). In a classic exercise study, three pigs (*Sus scrofa*) and one armadillo (*Dasypus novemcinctus*) were run on treadmills for 60 min a day for 3–6 months. After sacrifice, the exercised individuals were compared with their nonexercised sibling controls (identical sample sizes to the experimental groups). Lieberman reported a 10–60% increase in long bone cross-sectional dimensions of the load-bearing long bones of the runners, replicating the findings of

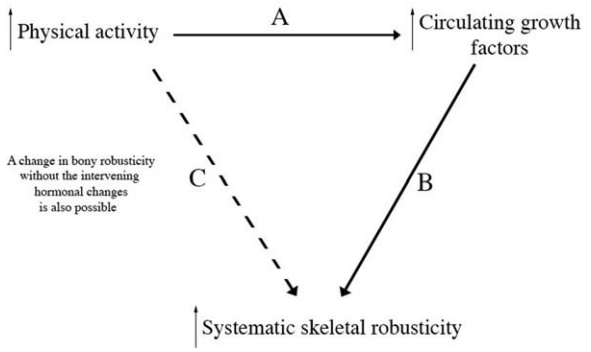

FIGURE 1 Simplified illustration of the systemic robusticity hypothesis (Lieberman, 1996). The current experiment was designed to test all three relationships. One specific covariate included in many of our statistical models was average food consumption at various times during the experiment, which we hypothesized may have had a local (rather than systemic) effect on CVT

many earlier exercise studies. Intriguingly, however, the exercised animals also showed 20–30% thicker cranial vault bones. However, cranial vault bones serve no a load-bearing function, therefore, no *a priori* reason exists for expecting them to increase in thickness as a response to load-bearing exercise. To explain this seemingly incongruent result, Lieberman hypothesized that because exercise releases growth hormones systemically (Lassarre, Girad, Durand, & Raynaud, 1974; Felsing, Brasel, & Cooper, 1992), greater cranial robusticity could be a simple response to the increase in Growth Hormone itself, or a related hormone, caused by exercise. He concluded that "the thick cranial vaults of most hunter-gatherers and early agriculturalists suggests that they may have experienced higher levels of sustained exercise relative to body mass than the majority of recent, postindustrial humans" (Lieberman, 1996: p. 217).

Since the publication of the SRH, it has been cited as the primary hypothesis to explain hypertrophy of cranial vault bones in *Homo erectus* in articles (Athreya, 2009; Bruner et al., 2017; Chirchir et al., 2015; Crevecoeur, Brooks, Ribot, Cornelissen, & Semal, 2016; Curnoe & Green, 2013; Davis, Windh, & Lauritzen, 2010; Tryon et al., 2015), textbooks (Conroy, 2005; Wolpoff, 1999), and in information written for the public (Lieberman, 2011). However, the proposed relationships among physical activity, hormone levels, and systemic skeletal robusticty have never been explicitly tested, which prompted our experimental design.

A simplified model of the SRH is depicted in Figure 1. Lieberman manipulated physical activity in his experimental models and observed an increase in systemic skeletal robusticity. He proposed an increase in circulating growth factors as the intervening causal link; but did not measure growth hormone in his experimental animals. Thus, in the present study, we used a model organism experimentally selected for high physical activity and measured that activity's relationship with circulating growth factors (relationship A), the relationship between those growth factors and skeletal robusticity (relationship B), and additionally tested the relationship between physical activity and skeletal robusticity (relationship C), given the possibility that growth hormones were not the primary causal factor for the observed increase in skeletal robusticity. Here we describe an experiment in which laboratory environmental conditions of the mouse (*Mus musculus*) were modified in an attempt to induce changes in cranial vault thickness. The mouse, due to small body size, short generation length, high fecundity levels, and relatively inexpensive care requirements, is a frequent model organism in experimental laboratories (Carlson & Byron, 2008). The structure of the mouse cranium is similar to that of primates in that it is trilaminar and has similar attachment sites for the temporalis and masseter muscles, the primary muscles of mastication (Hallgrímsson, Willmore, Dorval, & Cooper, 2004). In addition, our use of the unique High Runner (HR) mouse lines, allowed us to increase the levels of voluntary exercise much above those of ordinary mice (Copes et al., 2015; Garland, Zhao, & Saltzman, 2016; Swallow, Carter, & Garland, 1998; Wallace & Garland, 2016), in an attempt to imitate the increased activity of Lieberman's pigs and armadillos (1996), although the activity in the mice here was voluntary, while that in Lieberman's study was forced.

2 | MATERIALS AND METHODS

2.1 | Selection experiment background

The mice used in this experiment were from replicate lines that had been selectively bred over 57 generations for high voluntary exercise in the laboratory of Theodore Garland. Since 1993, four replicate lines bred for high voluntary wheel-running behavior, based on total revolutions on days 5 and 6 of a 6-day exposure to wheels (1.12-m circumference; Lafayette Instruments, Layfatette, IN) attached to standard housing cages (Swallow et al., 1998). The starting population was 224 individuals from the outbred, genetically variable, Hsd:ICR strain (Carter, Garland, Dohm, & Hayes, 1999), purchased from Harlan-Sprague-Dawley.

After two generations of random breeding in the laboratory, mice were randomly divided into one of eight lines, four bred for high running and four bred without regard to running and hence serving as controls, with each line maintained by 10 mating pairs per generation. The selection protocol has been consistent for all generations of the selection experiment, and relies on wheel revolutions that recorded daily in 1-min intervals by a photocell counter attached to the wheel and compiled through customized software by San Diego Instruments (San Diego, CA). In the four replicate HR lines, the male and female from each family with the most total revolutions on days 5 and 6 of a 6-day test, performed when the mice are ~6–9 weeks of age, were chosen to propagate the lines to the next generation. Within all control lines, breeders were paired randomly, with the exception that sibling matings were not allowed.

Wheel running by the four selected lines increased rapidly and reached apparent selection limits at generations 16–28, depending on sex and line (Careau, Wolak, Carter, & Garland, 2013), at which point they ran, on average, about 2.5–3 times as many revolutions per day than the four non-selected control lines, a difference that has remained approximately constant up to the present time (generation 57). The selected and control lines have been shown to differ in a number of behavioral and physiological traits, including, importantly for this study,

differences in skeletal morphology (e.g., Kelly, Czech, Wight, Blank, & Garland, 2006; Middleton et al., 2010; Schutz, Jamniczky, Hallgrímsson, & Garland, 2014; Wallace, Tommasini, Judex, Garland, & Demes, 2012; Wallace et al., 2011; Young, Hallgrimsson, & Garland, 2009).

2.2 | Experimental design

All experimental procedures were approved by the Institutional Animal Care and Use Committees at Arizona State University and the University of California, Riverside. A total of 100 females equally divided between selected and control lines were chosen from across the eight replicate lines, toe clipped for identification, and housed individually beginning at weaning (21–23 days of age). Half were housed in a cage with access to a wheel (described below), and half were housed in a cage without access to the wheel.

These are the same individuals as reported in Copes et al. (2015). The mice were all housed in a single room with constant temperature (22–23°C) and relative humidity (23–26%). The light/dark cycle was 12/12, with lights on at 07:00. Mice were provided with Teklad Harlan 8604 pelleted diet (24% protein and 3 kcal g^{-1}) and fresh tap water *ad libitum* and fresh cages and water bottles were provided every 2 weeks.

The 12 weeks of experimental procedures began when the mice were 24- to 27-days old. Mice wean at ~3 weeks, reach sexual maturity at 6 weeks, and experiments involving bony changes in mice typically last 8 to 12 weeks, as it has been shown that bony growth slows substantially after puberty (Jilka, 2013). Weekly procedures included weighing of each mouse and food hopper, from which apparent food consumption was determined (Swallow, Koteja, Carter, & Garland, 2001).

Multiple bone-labeling compound injected at known points throughout ontogeny allow for measures of early vs. late growth throughout the skeleton (Pautke et al., 2005). Although we do not present results of the growth analysis here, we report the procedures to present a complete account of all handling (invasive and otherwise) to which the mice were subjected. At the beginning of week 1 of the experiment, each mouse was injected with a fluorescent bone-labeling compound (alizarin red). Injections were repeated, alternating compounds among alizarin, xylenol orange or DCAF blue at the beginning of weeks 2, 3, 4, 10, 11, and 12. All three compounds chelate into the mineralizing front of the growing bones, leaving a colored ring easily observed via immunohistochemistry after histological preparation (Hoyte, 1960).

At the beginning of weeks 1 (at ~24 days of age), 3, 5, and 7, we collected ~75 μL of blood via the mandibular plexus (Hoff, 2000), and refrigerated overnight to ensure maximum clot formation. After centrifuging the blood samples at 13,300 RPM for 12 min at 4°C, the serum was collected and the clot discarded. Serum samples were kept at −80°C.

2.3 | Measuring activity

Both wheel running (for half of the sample given access to wheels) and spontaneous physical activity within the cage (for the entire sample) were measured throughout the experiment.

2.4 | Wheel running

At ~24 days of age, half of the mice were given access to the same wheels as used in the selection protocol attached to their cages (Swallow et al., 1998). Each of the four groups (Control with and without wheel access and HR with and without wheel access) began with 25 mice. For the remainder of the paper, we use the term Active to refer to the groups with access to wheels whereas those without access to wheels are referred to as sedentary. Each day, a computer recorded revolutions in each 1-min interval over a period of 23.5 hr. Following previous studies (e.g., Copes et al., 2015), we calculated the total number of revolutions, the number of 1-min intervals with at least one revolution (minutes of wheel activity), the mean speed of running (revolutions/intervals), and the single interval with the greatest number of revolutions (maximum speed) using SPSS (IBM).

2.5 | Spontaneous physical activity in the home cage

All 100 cages were fitted with a corner-placed, passive infrared sensor (Talon TL-Xpress-A; Crow Electronics, Fort Lee, NJ) housed in a wire-mesh protective enclosure (Copes et al., 2015). Connected to a digital I/O board (ICS 2313; ICS Electronics, Pleasanton, CA) interfaced to a Macintosh computer with custom software, the sensors have an ~90° field of view and a reset time following motion detection of 1–2 s. The software scanned each sensor approximately three times per sec and recorded sensor status as "1" (movement detected) or "0" (no movement detected). A mean value (0–1) was computed for each minute, with zero indicating no activity detected and one indicating activity detected during each of the ~180 scans per min. Mean values were saved to disk every 10 min. Pre-experiment tests indicated the capacity to detect even small movements (grooming, etc.) and that noise (i.e., false positives) was rare. Total home-cage activity (HCA) was taken as the sum of all activity over 23.5 hr. The number of 1-min intervals during which any HCA was registered was also recorded, and by dividing total HCA by minutes of activity, an estimate of mean intensity of HCA was calculated.

2.6 | Dissections and specimen preparation

The experiment lasted 12 weeks. Three mice died of various causes over the course of the experiment. At its conclusion, the remaining 97 mice were euthanized by CO_2 overdose followed by cardiac puncture (blood saved for hormone assay), and dissected for tissue collection. Tissues collected included the triceps surae muscles, the mass of which were used to determine the number of mice with the mini muscle phenotype (Kelly et al., 2013); 18 mice were found with the trait in this sample. Any tissue not harvested was removed either at dissection and discarded or was removed via soaking of the carcass in a 1% solution of enzymatic detergent (marketed as Tergazyme by Alconox).

2.7 | μCT scanning

The parietal, interparietal, and both dentaries (hemi-mandibles) of each specimen were μCT scanned using a Scanco CT40, Scanco Medical AG,

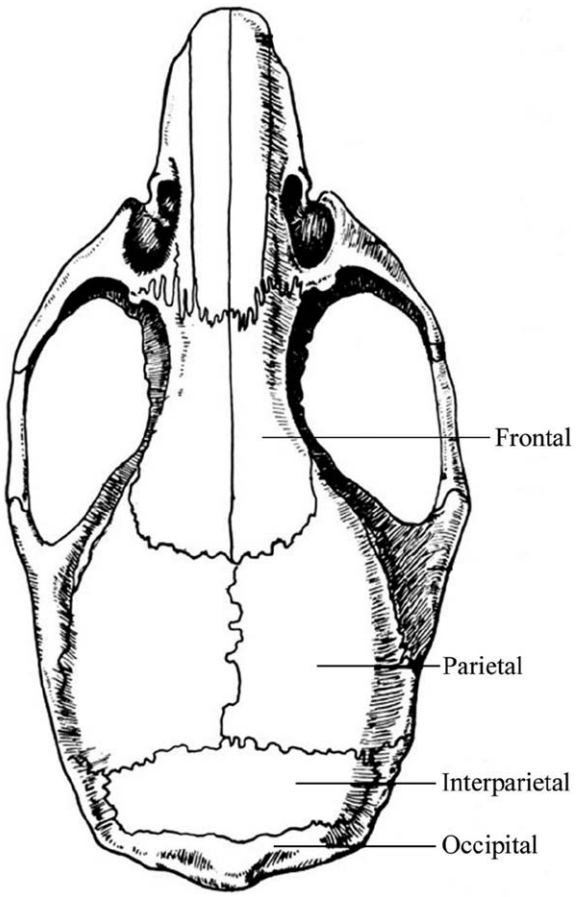

FIGURE 2 Dorsal view of mouse skull. The parietal and interparietal bones were harvested, μCT scanned, and their thickness measured for this analysis

Basserdorf, Switzerland) at Stony Brook University (24 μm resolution; 45 kV, 177 μA, 100-ms integration). The interparietal bone in mice is located between the parietals and occipital (Figure 2). We chose to measure the interparietal and parietal bone because they are the flattest bones of the mouse cranium without additional attached features that could not be included in a quantification of cranial vault thickness (i.e., the petrous portion of the temporal bone, the supraorbital ridges of the frontal bone, and the foramen magnum of the occipital bone).

The right femur and humerus were μCT scanned at the University of Calgary (Viva-CT40, Scanco Medical AG, Basserdorf, Switzerland) at 21-μm resolution (55 kV, 145 μA, 500 projections). The femur and humerus were chosen because they are the largest long bones with the greatest attached muscle mass, and are the most frequently examined in studies of the effects of exercise on bone morphology (Ferguson, Ayers, Bateman, & Simske, 2003; Jepsen et al., 2009; Judex et al., 2004; Tommasini, Wearne, Hof, & Jepsen, 2008; Yang et al., 2007).

The postcranial scans were analyzed using an automated algorithm that measured total area, cortical area, cortical thickness, and measures of bending strength (I_{min}, I_{max}, J) for a 50 slice (1.2 mm) stack centered in the midshaft of each bone (Lublinsky, Ozcivici, & Judex, 2007).

Using a similar automated algorithm, written specifically for this project, mean, median, and maximum thickness of the entire interparietal and parietal bones, along with mean thickness of the trabecular and cortical portions separately were calculated (Figure 3).

The cranial vault thickness algorithm automatically finds the boundary between bone and air using the voxel brightness, assigned based on attenuation, or the amount of X-ray energy the material absorbs. The Scanco μCT system converts individual attenuation measurements into Hounsfield units (which quantify radiodensity) by comparing specimen absorption values to a standard calibration phantom provided by the manufacturer (http://www.scanco.ch/index.php?id=faq_general#c926). The algorithm then detects the bone–air boundary using an automated thresholding paradigm (Lublinsky et al., 2007).

The algorithm measures the thickness of the total bone and then masks the trabecular bone (diploë) and calculates its thickness. Measuring thickness in microCT scans of bones was first validated by Müller et al. (1996). The cortical–trabecular boundaries are calculated using an automated thresholding paradigm, identical to the process used for detecting cortical–trabecular boundaries in postcranial bones, which has been validated in many studies (e.g., Lublinsky et al., 2007). Thickness is calculated using a sphere-fitting method, by which the diameters of the largest possible spheres that can be fitted through each voxel that is completely contained within the layer boundaries are calculated and averaged across the entire layer (Bouxsein et al., 2010). The sphere-fitting method is advantageous in that the orientation of the bone within the scan does not affect the thickness measure, whereas orientation is essential to replicate if linear measurements are used.

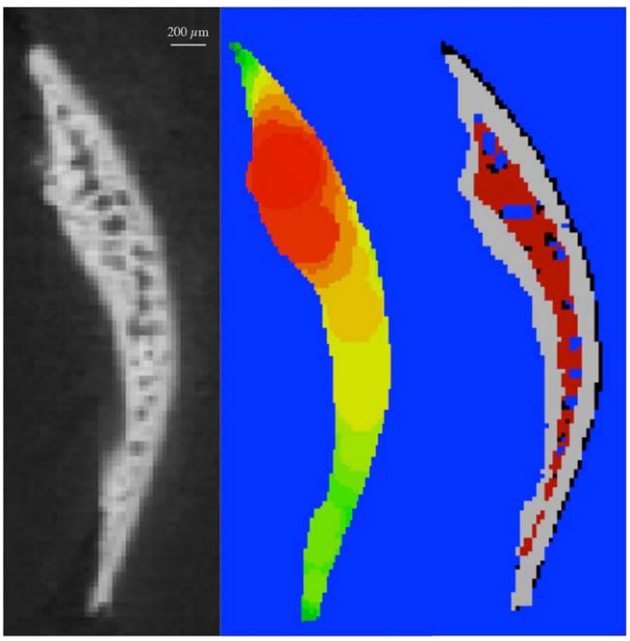

FIGURE 3 An example of an interparietal bone microCT scan (left) analyzed using the algorithm written specifically for this study. The algorithm measured total bone thickness (middle; warmer colors indicate thicker areas) and reported mean thickness for each specimen. The algorithm also detected the boundaries between the cortical shell and inner diploë layers and reported average thickness of the diploë

The results reported by the algorithm include mean total thickness of bone, as well as mean thickness of the diploë layers. We calculated mean cortical thickness by subtracting mean diploë thickness from mean total thickness. Confidence that the resolution of the scans was adequate to accurately measure both total CVT and diploë thickness is based on the fact that the minimum ratio of voxel size to thickness of structures required for accurate measurement is 2:1 (although the ideal is ratio is 5:1 (Bouxsein et al., 2010). Across our sample, the average ratio between voxel size and diploë thickness (the smallest measurement of interest) is 3.9:1.

2.8 | Linear measurements

To measure long bone length and several dimensions of the mandible, still images of the bones were necessary. The right femur, both humeri, and both dentaries were placed on a flatbed scanner and imaged in 24-bit color at 1,200 dots per inch (TIFF format without file compression). This method has similar characteristics to camera-based two-dimensional imaging systems, but with the added benefit of ease of setup, portability, and low equipment cost (Young et al., 2009). Although parallax is an issue with all optical systems, this error is most prevalent in flatbed scanners when objects extend a large distance from the image sensor. The small size of the mouse bones limited this error. To further minimize the possibility of scanner error, the bones were scanned twice to create two separate image files. Two-dimensional landmark data were collected twice from each of the two scanned images using ImageJ (http://rsbweb.nih.gov/ij/); measurements were made by a single observer. The four measurements of femur and humerus length were subsequently averaged across scans and trials. Mandible size was calculated as a geometric mean of corpus height, ramus height, and length, which was then averaged across the scans and trials.

2.9 | ELISA hormone assays

Lieberman (1996) hypothesized that growth hormone (GH) might be the causal link between exercise and increased cortical thickness in his experimental animals. In rodents, as in many mammals, diurnal fluctuations in the pattern of GH secretion make it difficult to measure without temporally dense and frequent sampling from which to establish baseline levels (Bernstein, Leigh, Donovan, & Monaco, 2007; Bidlingmaier & Freda, 2010; Gabriel, Roncancio, & Ruiz, 1992; Ionescu & Frohman, 2006) Thus, blood samples taken from the mice at the conclusion of the experiment were analyzed for Insulin-like Growth Factor 1 (IGF-1) and Insulin-like Growth Factor Binding Protein 3 (IGFBP-3). The ratio between IGF-1 and IGFBP-3 has been shown to be a time-stable proxy for circulating GH levels (Bernstein et al., 2007). The hormone levels were measured from the final blood sample taken at sacrifice using enzyme-linked immunosorbant assay (ELISA). Kits were purchased from Alpco and the analyses were performed by the Endocrinology Lab in the Orthopaedics Department at Yale University. Because of the circadian rhythm of GH secretion, we included kill time as a possible covariant in statistical models of our hormone values, even though IGF-I and IGFBP-3 are not known to have strong circadian rhythms (Baumann, 2005; Beamer, Donahue, & Rosen, 2000; Butler & Le Roith, 2001; Clemmons, 2007; Giustina, Mazziotti, & Canalis, 2008).

2.10 | Statistical analysis

The nature of the selection experiment requires that effects of linetype (HR vs. control) are tested over the variance among replicate lines (the experimental unit), which are random effects nested within a fixed effect. Degrees of freedom for this main effect are 1 and 6, regardless of the number of mice studied. In addition, effect of activity (wheel access or not) and the interaction between linetype and activity environment are also tested over the variance among lines or the activity*-line interaction, again with 1 and 6 d.f. Thus, following numerous previous studies of these lines of mice, data were analyzed as covariance models in SAS Procedure Mixed, with REML estimation and Type III Tests of Fixed Effects. Statistical significance was judged at $p \leq 0.05$. Main effects were linetype (selected vs. control), activity (active vs. sedentary), and the mini-muscle phenotype (Garland et al., 2002). The mini-muscle phenotype is caused by a Mendelian recessive mutation (Kelly et al., 2013) that halves hindlimb muscle mass, with many pleiotropic effects, including lengthening the hindlimb bones and altering their linear breadths (e.g., Kelly et al., 2006). The phenotype has been fixed in one HR line, and is polymorphic in another. It has not been observed in two of the four HR lines or any of the C lines. Covariates included $\log_{10}$ body mass at sacrifice, average food consumption (see calculation below), and IGF-1, IGFBP-3, and their ratio measured in the blood sample drawn at sacrifice. Outliers were removed from each model if the absolute value of their studentized residual was >3 (Littell, Milliken, Stroup, Wolfinger, & Schabenberger, 2006).

As mentioned earlier, we measured the mass of food each mouse consumed each week. We then regressed each mouse's weekly apparent food consumption on its average body mass for that week (for example, [day7mass − day0mass]/2 gave us average mouse body mass for experimental week 1) and calculated each individual's residual from the mean. The calculations were repeated for each week of the experiment. We then averaged each mouse's twelve residual values to determine an experiment-wide quantification for body mass-adjusted food consumption relative to other mice. This average was also used as a covariate in some models, so we could investigate if food consumption had a localized effect on cranial vault thickness apart from the effects of exercise or hormone levels (cf., Figure 1). Finally, we also calculated the body mass-adjusted food consumption average for the first 4 weeks of the experiment (during which the mice were still growing rapidly) and the last 8 weeks of the experiment (after the mice had reached sexual maturity and their bone growth had slowed) in order to compare early and later food consumption.

3 | RESULTS

3.1 | Body mass

Models examining the effects of activity, linetype, their interaction, and the mini-muscle phenotype on body mass at Day 0 and at sacrifice are

TABLE 1 *p*-values of mixed model ANCOVA analyses examining the effects of linetype (high runner vs. control), activity (active vs. sedentary), their interaction, and mini-muscle phenotype on total body mass (g) at the start and end of the 12-week experiment

Trait	N	Linetype; df = 1,6	Activity; df = 1,6	Act*Ltp; df = 1,6	Mini muscle; df = 1, 70–80
Day 0 mass	100	0.3327	0.5161	0.9357	0.6981
Mass at sacrifice	97	0.0939	0.0923	0.5230	0.4308
Mass at sacrifice[a]	97	0.0260 C>HR	0.0091 S>A	0.6596	0.2550
Mass at sacrifice[b]	94	0.0961	0.0914	0.5096	0.4665

[a]Mean food consumption weeks 1–12 included as a covariate.
[b]IGFI: IGFBP3 ratio included as a covariate.

given in Table 1, which provides all the covariates. Mice from the HR lines were, on average, slightly smaller than C mice (mouse mass at the start of the experiment [mean age = 26.8 days] was 15.9 ± 0.6 g [LSM ± SE] for HR vs. 16.8 ± 0.8 g for C; $p = .33$). However, at the start of the experiment, there was no significant difference in body mass between mice assigned to the wheel group (16.2 ± 0.6g) versus the non-wheel group (16.5 ± 0.6 g; $p = .5$); each activity group contains mice from both C and HR lines.

By the conclusion of the experiment, C mice were larger than HR mice when no covariates were included in the model, although not significantly so (27.3 ± 1.3 g vs. 24.4 ± 1.12 g; $p = 0.09$ respectively; Figure 4). In the same model, sedentary mice were not significantly larger than active mice (26.5 ± 0.9 g vs. 25.3 ± 0.9 g; $p = 0.5$), regardless of linetype and the interaction between linetype and activity was not significant. When including mean food consumption over the 12-week experiment as a covariate, the linetype and activity differences became significant, although the interaction between the two remained nonsignificant (C = 27.9 ± 1.06 g > HR = 23.9 ± 0.90 g, $p = .026$; S = 27.19 ± .78 g > A = 24.65 ± 0.82 g, $p = .009$). The inclusion of the hormone ratio into the model rendered both activity and linetype nonsignificant, although the differences in mass were in the same direction as the other models. Mini-muscle was not a significant factor in any model of body mass, regardless of covariates.

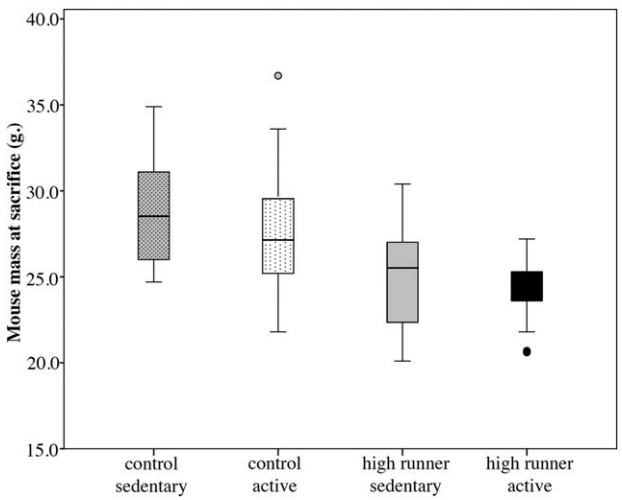

FIGURE 4 Raw measures of mouse body mass at the end of the experiment. Mouse mass at sacrifice was significantly associated with linetype (mice from the selectively bred high runner lines are smaller), but not with access to wheels for 12 weeks (activity). Values shown are medians (central horizontal bars) surrounded by the interquartile range (upper and lower box limits). The whiskers encompass the minimum and maximum values excluding outliers, defined as data points more than two box lengths above the 75th or below the 25th centile, which are shown as individual data points

3.2 | Activity differences

As expected, Active HR mice ran significantly further than Active C mice each week, due to both longer duration of running and higher average speed of running (Figure 5; see also Copes et al., 2015). Full results of weekly average activity parameters are provided in the Supporting Information (Table S1).

Active mice had lower home-cage activity than Sedentary mice, which is logical given that they spent time out of their cage running on the provided wheel (Figure 6). Linetype, however, also impacted home cage activity–Sedentary HR mice had significantly higher levels of home-cage activity than Sedentary C mice throughout the course of the experiment, due to moving during more intervals each day. Among Active mice, linetype did not have a significant effect on home-cage activity measures.

3.3 | Hormones

The relationship between activity and hormones was tested to investigate if high levels of voluntary exercise caused increases in the ratio of IGF-1 to IGFBP-3. Analyzed individually, IGF-I and IGFBP-3 were unrelated to activity, linetype, or their interaction, whether or not time of sacrifice was included as a covariate (Table 2). The ratio of IGF-I to IGFBP-3 does vary by linetype (Figure 7). However, C mice had significantly higher ratios than HR mice and coupled with the fact that hormone levels did not vary with activity, the direction of linetype difference in the hormone ratio does not support the hypothesis that increased activity (either via selection or daily activity alterations) caused an increase in circulating growth hormones.

3.4 | Cranial vault thickness

Eighteen models were compared to test the effects of activity, linetype, and their interaction on each measurement of cranial vault thickness

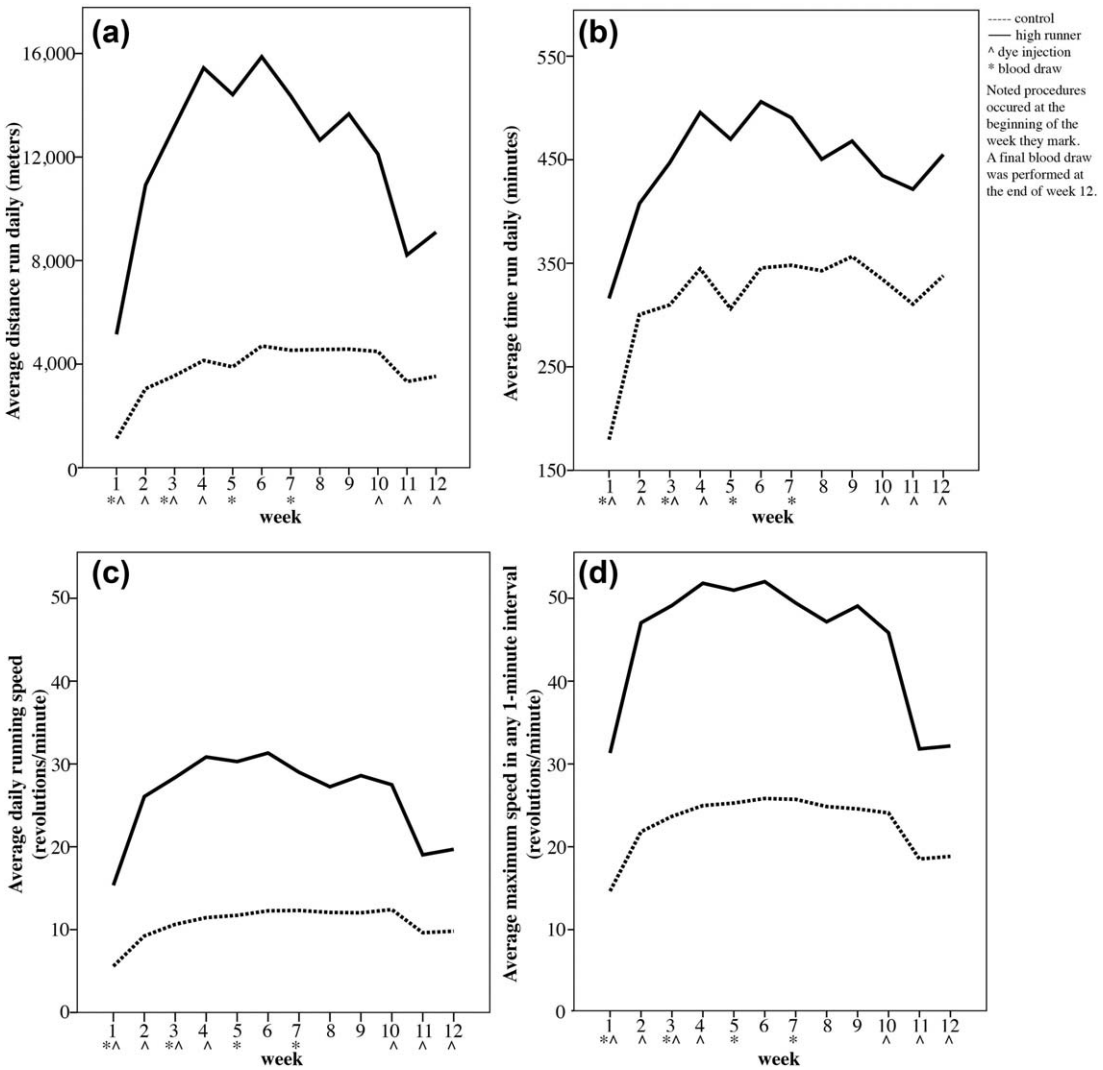

FIGURE 5 Running activity by linetype (C vs. HR) over the course of the 12-week experiment. (a) Average daily distance run in meters. (b) Average time spent running per day in minutes. (c) Average daily running speed. (d) Average maximum speed in any 1-min interval

(Table 3). Models were run including three separate measures of average food consumption (early, late, and total), as well as the ratio of IGF-I/IGFBP-3 as covariates. In only one model did linetype or activity have a statistically significant effect on cranial vault thickness: HR mice had significantly thicker interparietal bones than C mice only when total food consumption was included in the model as a covariate (least square means ± SE: HR: 0.303 ± 0.009 mm; *C*: 0.269 ± .010 mm; p =.046; Figure 8a). However, in the other 17 models, cranial vault thickness did not vary with activity, linetype, or their interaction, regardless of covariates used (see Figure 8b for an example).

3.5 | Postcranial robusticity

No measures of femoral or humeral robusticity were significantly associated with either activity, linetype, or their interaction, whether or not hormone levels were included as covariates (Table 4). As expected, postcranial robusticity covaried positively with body mass, and mice with the mini-muscle phenotype had significantly lower femoral cortical areas and bending moments of inertia than nonmini-muscle mice (non-mini FCA = 0.89 ± 0.03, mini FCA = 0.76 ± 0.05, p = .006; non-mini FJ = .36, mini FJ = 0.27, p = .0002).

We also tested the relationships among measures of postcranial robusticity and CVT (total and cortical thickness) with linear regression (using the entire sample and each of the four groups separately). Pairs in which the r^2 of the regression was >.3 were considered significant for this analysis (Table 5). We did not find a consistent pattern. Total interparietal thickness was not significantly associated with any measure of postcranial robusticity. Interparietal cortical thickness was significantly associated with total femoral cross-sectional area, femoral polar moment of inertia, and humeral length, but only within the Sedentary C line mice. Both Active and Sedentary C line mice showed a relatively strong relationship between total parietal thickness and all measures of postcranial robusticity, but HR line mice did not have a significant relationship between parietal thickness and any measure of postcranial robusticity. Finally, parietal cortical thickness was

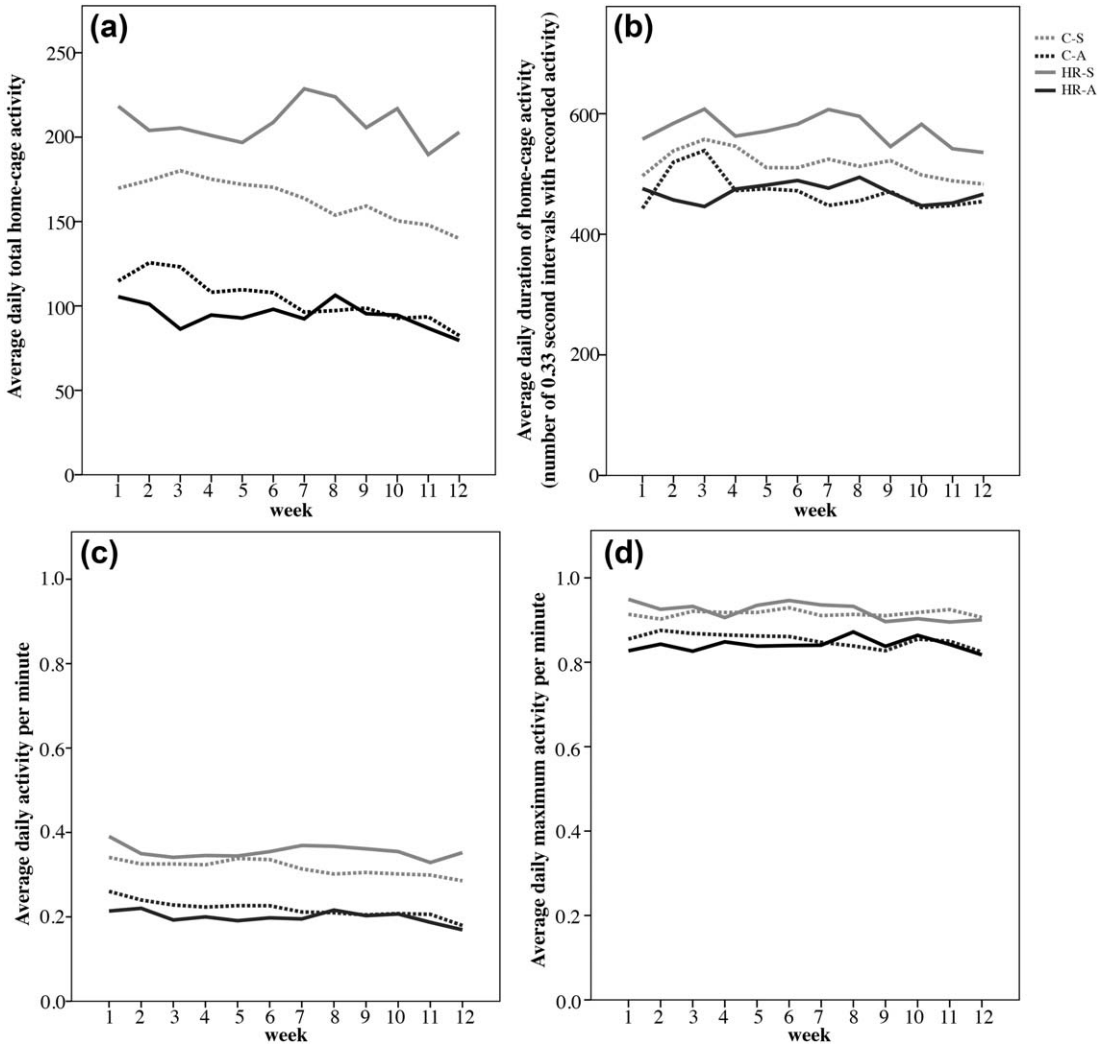

FIGURE 6 Measure of home-cage activity over the course of the experiment. (a) Average total summed activity (23.5 hr per day). (b) Average number of 0.3 s intervals with any recorded activity. (c) Average activity per 1-min interval. (d) Average maximum activity in each 1-min interval. C–S: Control line, no wheel access (sedentary); C–A: Control, with wheel access (active); HR–S: High runner line, sedentary; HR–A: High runner, active

significantly associated with total femoral cross-sectional area, but again, only in Sedentary C line mice.

3.6 | Food consumption

One possible intervening variable linking physical activity and increased CVT is food consumption. We expected active mice to eat more than sedentary mice and thought it possible that increased mastication might have an independent effect on CVT. Average food consumption is illustrated in Figure 9. Once weekly food consumption was adjusted for body mass as described above, group averages were totaled in three ways—early consumption for the first 4 weeks, late consumption for weeks 5 through 12, and total consumption for the full 12 weeks of the experiments. In the first 4 weeks of the experiment, both activity

TABLE 2 *p*-values of mixed model ANCOVA analyses examining the effects of linetype (high runner vs. control), activity (active vs. sedentary), their interaction, and mini-muscle phenotype on hormone levels at the end of the 12-week experiment

Trait	*N*	Linetype; df = 1,6	Activity; df = 1,6	Act*Ltp; df = 1,6	Mini muscle; df = 1, 70–80
IGF-1	94	0.3270	0.1878	0.0778	0.1583
IGFBP-3	94	0.3574	0.5734	0.3931	0.9715
IGF-1 : IGFBP-3 ratio	94	0.0193 C>HR	0.6281	0.2750	0.0120

The significance or lack thereof did not change in any model when including time of sacrifice as a covariate.

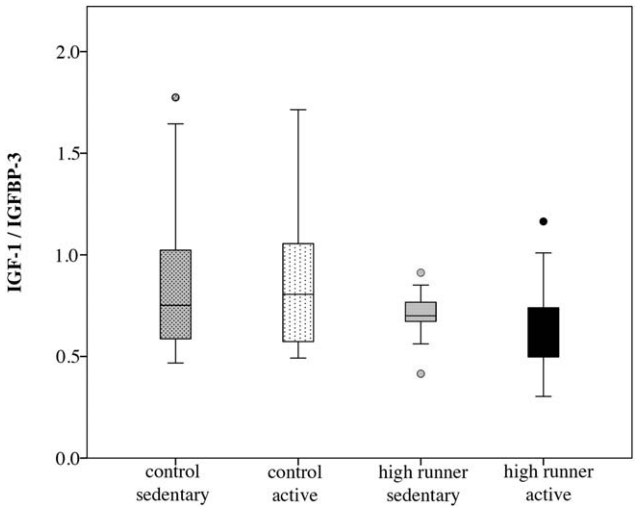

FIGURE 7 Raw values for the IGF ratio obtained from the blood sample taken at sacrifice. Activity (access to wheels for 12 weeks) is a significant effect, with control mice showing significantly higher ratios than high runner mice (opposite of the predicted relationship). Graph parameters as in Figure 4

and the interaction of activity and linetype significantly predicted food consumption: Mice with wheels ate significantly more than mice without ($p < .001$), and high runner mice with wheels ate significantly more than other groups ($p = .007$; Table 6). These differences persisted in the second part of the experiment after mice reached sexual maturity and when food consumption across the entire 12-week study was analyzed. Reductions in food consumption at weeks 3, 7, and 11 are coincidental with procedures performed on the mice at the beginnings of those weeks, but similar procedures performed at the beginnings of weeks 2, 4, 5, 10, and 12 did not coincide with a similar reduction in food consumption.

4 | DISCUSSION

We describe here one of the first experiments designed to test the relationships among exercise, hormones, and cortical bone outlined in the systemic robusticity hypothesis (Lieberman, 1996). We also measured food consumption as a possible mediating influence on cranial vault thickness. Our results provide no support for the SRH either as a whole or for its component parts (Figure 1). We did find significant

TABLE 3 *p*-values of mixed model ANCOVA analyses examining the effects of linetype (high runner vs. control), activity (active vs. sedentary), their interaction, and mini-muscle phenotype on various measures of cranial vault thickness

Trait	*N*	Linetype; df = 1,6	Activity; df = 1,6	Act*Ltp; df = 1,6	Mini muscle; df = 1, 70–80	Bodymass at sacrifice; df = 1, 70–76
Interparietal—total thickness	91	0.1792	0.4643	0.6013	0.4603	0.1761
Interparietal—total thickness[a]	91	0.0461 HR>C	0.4085	0.9471	0.2698	0.0177
Interparietal—total thickness[b]	89	0.1783	0.4849	0.7160	0.6016	0.1911
Interparietal—cortical thickness	91	0.6170	0.1363	0.8605	0.9552	0.0248
Interparietal—cortical thickness[a]	91	0.2200	0.9642	0.5643	0.8526	0.0042
Interparietal—cortical thickness[b]	89	0.6106	0.1537	0.7221	0.8070	0.0299
Interparietal—diploë thickness	91	0.1764	0.3888	0.1722	0.3905	0.4150
Interparietal—diploë thickness[a]	91	0.1016	0.1773	0.3142	0.2884	0.8447
Interparietal—diploë thickness[b]	89	0.1644	0.3694	0.1809	0.3991	0.4270
Parietal—total thickness	94	0.6162	0.6635	0.1758	0.0552	<0.0001
Parietal—total thickness[a]	94	0.7341	0.9578	0.2257	0.0521	<0.0001
Parietal—total thickness[b]	92	0.4253	0.6835	0.2426	0.0528	<0.0001
Parietal—cortical thickness	93	0.3602	0.0794	0.9380	0.6028	0.0003
Parietal—cortical thickness[a]	93	0.1590	0.6760	0.7522	0.4485	0.0001
Parietal—cortical thickness[b]	91	0.2847	0.0950	0.7777	0.9556	0.0004
Parietal—diploë thickness	93	0.3091	0.1228	0.2910	0.3390	0.0235
Parietal—diploë thickness[a]	93	0.1621	0.7220	0.1941	0.4580	0.1423
Parietal—diploë thickness[b]	91	0.1683	0.1343	0.2065	0.1679	0.0185

In the cases in which body mass at sacrifice was associated with CVT, the effect was always positive.
[a]Mean food consumption weeks 1–12 included as a covariate.
[b]IGFI: IGFBP3 ratio included as a covariate.

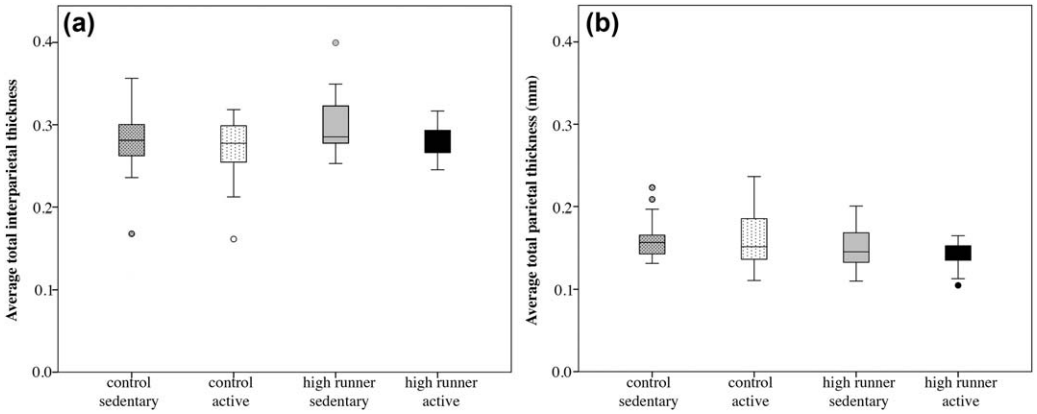

FIGURE 8 Raw values for cranial vault thickness of the interparietal (a) and parietal (b) bones. HR mice had significantly thicker interparietal bones than C mice only when total food consumption was included in the model as a covariate (see Table 3). Activity, however, was not a significant factor. No differences in parietal thickness were found in any statistical model. Graph parameters as in Figure 4

differences in the amount of food consumed by each group, but as we were unable to replicate Lieberman's results of significant differences in CVT in active versus sedentary groups, the food consumption difference may not be relevant—if CVT had differed significantly among groups, then the food consumption variation may have been a biologically significant finding; however, in the absence of CVT differences, the food consumption differences do not suggest that localized mastication forces (as opposed to systemic hormone levels) significantly impacted CVT.

The use of mice as a model, although extremely common, limits the conclusions we can draw from our results. Mice are smaller than the armadillo and pig models Lieberman (1996) used (and much smaller than human ancestors), and it is possible that activity did influence CVT, but our measurement resolution was insufficient to detect any differences due to imaging limitations. Nano-CT may be required to appreciate small variation in mouse skeletal robusticity. Allometric effects might result in mouse bones differing from the bones of larger mammals in terms of their response to exercise, hormones, or feeding. Mice are also generally considered somewhat "overbuilt" skeletally (Rubin & Lanyon, 1984) which may also limit the ability to induce bony changes via mechanisms like exercise, although small and large mammals seem to have relatively consistent bone and muscle stresses due to modification of postures (Biewener, 2005).

That said, many prior studies have documented variation in postcranial robusticity in mice (whether induced through exercise studies or not), measured successfully using micro-CT (Cosman, Sparrow, & Rolian, 2016; Green, Richmond, & Miran, 2012), suggesting that the measuring modality is adequate to detect typical bone morphology changes in mice. Specifically using mice from this selection protocol, Kelly et al. (2006) found that 8 weeks of wheel access did increase masses of the tibiafibula and foot bones in male mice, and Schutz et al. (2014) found significant differences in semicircular canal shape. However, the fact that we were unable to detect differences in measures of postcranial robusticity by activity in this experiment is concordant with the findings of Wallace et al. (2012), who failed to find exercise-induced differences in mid-diaphyseal bone area or area moments in a group of male mice from this same selection protocol. These varying results underscore the importance of a unified definition of "robusticity," as different measurement protocols are unsurprisingly linked to different conclusions.

It is also possible that the selection for endurance running affects the mechanosensitivity of the postcrania, and that the behavior of the mice does not allow for adequate rest or energetic resources to build the bony strength Wolff's Law would predict (Middleton et al., 2010). Work done by Jepsen's lab also suggests that mechanosensitivity of

TABLE 4 *p*-values of mixed model ANCOVA analyses examining the effects of linetype (high runner vs. control), activity (active vs. sedentary), their interaction, and mini-muscle phenotype on the size and robusticity measures of the femur and humerus

Trait	*N*	Linetype; df = 1,6	Activity; df = 1,6	Act*Ltp; df = 1,6	Mini muscle; df = 1, 70–80	Body mass at sacrifice; df = 1, 70–76
Femur—length	95	0.8074	0.7977	0.9378	0.6004	<0.0001
Femur—cortical cross-sectional area	93	0.5984	0.6464	0.6744	0.0061 non-MM > MM	<0.0001
Femur—polar moment of inertia	93	0.0598	0.9599	0.9046	0.0002 non-MM > MM	<0.0001
Humerus—length	95	0.8912	0.4992	0.1675	0.6200	<0.0001
Humerus—cortical cross-sectional area	93	0.8778	0.6565	0.3940	0.0649	<0.0001
Humerus—polar moment of inertia	93	0.4656	0.7273	0.3059	0.1212	<0.0001

In every model, body mass at sacrifice was positively associated with postcranial size/strength.

TABLE 5 Linear regression parameters for analyses of cranial vault thickness and measures of postcranial size and robusticity

		Femoral length		Femoral total cross-sectional area		Femoral cortical cross-sectional area		Femoral polar moment of inertia	
		slope	r^2	slope	r^2	slope	r^2	slope	r^2
Interparietal total thickness (mm)	Combined	6.56E-03	0.012	0.03	0.02	0.02	0.004	0.06	0.02
	C S	0.03	0.167	0.11	0.21	0.09	0.055	0.21	0.157
	C A	−0.02	0.121	−0.02	3.74E-05	3.57E-03	1.46E-04	9.58E-03	5.00E-04
	HR S	0.03	0.263	0.05	0.066	0.14	0.16	0.15	0.115
	HR A	−3.90E-03	0.015	−0.03	0.078	−8.96E-03	0.003	−0.05	0.044
Interparietal cortical thickness (mm)	Combined	6.20E-03	0.062	0.03	0.11	0.04	0.109	0.07	0.124
	C S	0.02	0.279	0.07	0.391*	0.07	0.194	0.13	0.332*
	C A	−2.39E-03	0.01	0.01	0.029	0.02	0.028	0.03	0.032
	HR S	6.91E-03	0.132	1.58E-03	7.79E-04	0.03	0.067	0.01	0.009
	HR A	8.32E-05	1.90E-05	8.42E-03	0.02	0.03	0.1	0.03	0.037
Parietal total thickness (mm)	Combined	0.02	0.259	0.06	0.248	0.1	0.28	0.16	0.287
	C S	0.03	0.422*	0.1	0.568*	0.12	0.307*	0.2	0.515*
	C A	0.03	0.405*	0.11	0.483*	0.18	0.558*	0.25	0.537*
	HR S	0.01	0.086	−0.01	0.012	−6.84E-04	7.59E-06	−0.03	0.008
	HR A	4.08E-03	0.032	0.03	0.139	0.05	0.171	0.07	0.138
Parietal cortical thickness (mm)	Combined	6.16E-03	0.099	0.02	0.086	0.02	0.062	0.04	0.087
	C S	9.20E-03	0.266	0.03	0.334*	0.03	0.14	0.06	0.275
	C A	6.91E-03	0.087	0.02	0.102	0.04	0.098	0.06	0.117
	HR S	3.05E-03	0.027	−7.45E-03	0.013	−4.46E-03	0.001	−0.02	0.012
	HR A	3.29E-03	0.049	0.01	0.079	0.02	0.04	0.03	0.066
		Humeral length		Humeral total cross-sectional area		Humeral cortical cross-sectional area		Humeral polar moment of inertia	
		slope	r^2	slope	r^2	slope	r^2	slope	r^2
Interparietal total thickness (mm)	Combined	0.01	0.03	0.01	7.63E-04	8.46E-03	1.62E-04	5.00E-02	7.80E-04
	C S	0.04	0.189	0.22	0.108	0.38	0.141	0.93	0.126
	C A	−3.50E-03	0.018	−0.07	0.037	−0.16	0.057	−0.33	0.033
	HR S	0.04	0.246	0.02	0.037	0.25	0.074	0.33	0.02
	HR A	−2.90E-03	0.005	−0.05	0.045	−2.85E-03	7.00E-05	−0.13	0.018

(Continues)

TABLE 5 (Continued)

		Humeral length		Humeral total cross-sectional area		Humeral cortical cross-sectional area		Humeral polar moment of inertia	
		slope	r^2	slope	r^2	slope	r^2	slope	r^2
Interparietal cortical thickness (mm)	Combined	9.49E-03	0.114	0.05	0.051	0.07	0.054	0.21	0.063
	C S	0.02	0.308*	0.12	0.174	0.21	0.229	0.51	0.213
	C A	2.56E-03	0.018	−0.02	0.007	−0.05	0.032	−0.08	0.009
	HR S	7.78E-03	0.101	−7.63E-03	0.002	0.06	0.05	0.02	9.57E-04
	HR A	−8.85E-04	0.001	0.05	0.119	0.06	0.099	0.22	0.148
Parietal total thickness (mm)	Combined	0.02	0.251	0.14	0.172	0.24	0.299	0.67	0.255
	C S	0.03	0.425*	0.11	0.103	0.22	0.168	0.5	0.131
	C A	0.03	0.432*	0.25	0.309*	0.41	0.566*	0.98	0.396*
	HR S	0.01	0.046	0.07	0.035	0.11	0.029	0.4	0.045
	HR A	−1.39E-04	2.12E-05	0.09	0.305*	0.12	0.245	0.35	0.339*
Parietal cortical thickness (mm)	Combined	6.22E-03	0.068	0.03	0.023	0.05	0.059	0.13	0.039
	C S	9.69E-03	0.193	0.03	0.028	0.08	0.129	0.14	0.058
	C A	6.14E-03	0.052	0.02	0.005	0.06	0.047	0.11	0.019
	HR S	5.57E-04	4.24E-04	1.69E-03	8.26E-05	0.05	0.027	0.05	0.004
	HR A	4.48E-03	0.05	0.03	0.086	0.04	0.052	0.13	0.083

Cells with asterisks indicate relationships with r^2 values >0.3.

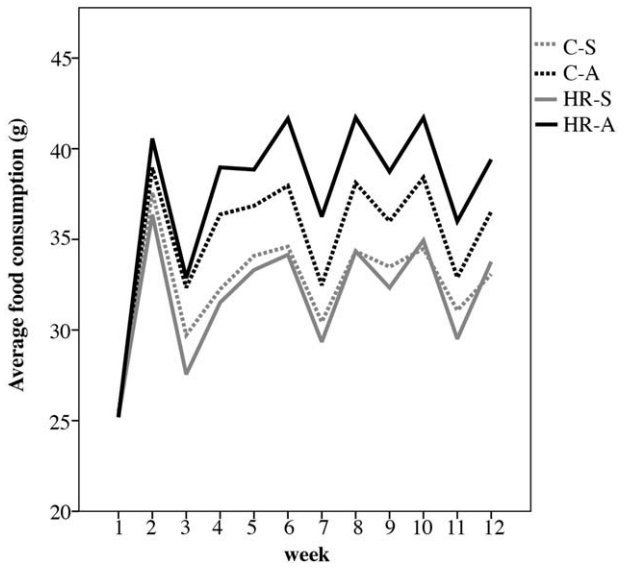

FIGURE 9 Average food consumption per group by week in grams. While food consumption was adjusted for average weekly body mass (see text) for use in the mixed model analyses, the data present in this figure are raw, unadjusted values. Note that HR mice are smaller in body mass, which means they eat less all else being equal. However, on an absolute basis, they eat similar amounts of food to C mice when housed without wheels, and more than C mice when housed with wheel access

bone varies by genetic background in mice (Jepsen, 2011; Price, Herman, Lufkin, Goldman, & Jepsen, 2005; Tommasini, Nasser, Hu, & Jepsen, 2007; van der Meulen, Jepsen, & Mikic, 2001), and it is possible that the Hsd:ICR strain used to begin the HR mouse selection experiment may be one with relatively mechanically insensitive bones. All of these factors could be manipulated in future tests of the SRH.

Additionally, the mice in this study in the exercise groups were given free access to wheels, whereas the animals in Lieberman's study (1996) were forced to run on treadmills. Forced exercise may be stressful and may also have changed circulating hormone levels (Brown et al., 2007; Yanagita et al., 2007) and had an effect on bony morphology that we were unable to replicate due to the animals in our study only undertaking voluntary exercise. Treadmill running also likely uses different muscles and causes different ground reaction forces than wheel running (cf., van Ingen Schenau, 1980), which may be more akin to climbing, with forelimb forces dominating.

Our method of collecting blood for hormone analysis did not result in adequate volumes to analyze hormone levels during the experiment. Thus, our hormone data come only from the blood collected at sacrifice. Given that all the animals showed an overall decrease in activity toward the end of the experiment (Figure 5), it is possible that we missed significant hormonal differences that occurred earlier and would have had a larger effect on skeletal development. Future work should be set up to more carefully measure longitudinal hormone data.

Although our experimental design was designed to identify correlations among physical activity, hormone levels, and skeletal robusticity, true causation would be more difficult to establish. However, multiple genetic mutant mouse strains with various knock-outs to the growth hormone axis are available (Al-Regaiey, Masternak, Bonkowski, Sun, & Bartke, 2005; Eckstein et al., 2002; Ramirez-Yañez, Smid, Young, & Waters, 2005; Schilling et al., 2001; Young et al., 2004). Future work will examine the effects of increased or decreased physiological levels of growth hormone on skeletal robusticity. Additionally, pharmacological manipulation of growth hormone may impact CVT and postcranial robusticity in interesting ways, which we plan to explore in the future.

Others have proposed several different ways to test the Systemic Robusticity Hypothesis. The fact that CVT and postcranial robusticity were not strongly correlated with one another is an interesting finding that has been reported within a small human sample and within two different species of nonhuman primate (Copes, 2012) and replicated within a larger sample of humans from multiple populations (Baab et al., submitted). Even without measuring physical activity or hormone levels, the Systemic Robusticity Hypothesis necessarily predicts a strong relationship among thickness measurements of cortical bone across the skeleton, a prediction not supported by our results.

Additionally, Eisová et al. (2016) hypothesized that a systemic effect of exercise could only increase CVT through expanded blood flow to the bone, which might cause expansion of the middle meningeal and diploic vessels. They found no correlation between parietal thickness and the size of the major vascular channels supplying the bone in a sample of modern human skulls. We did not measure vascular size of the mice in this experiment, but future analyses could examine heart ventricle mass or the size of nutrient canals in the long bones to attempt to replicate Eisova et al.'s results. Heart ventricle mass (adjusted for body mass) is known to be larger in HR mice than in C, and also to increase with several weeks of wheel access, including in

TABLE 6 *p*-values of mixed model ANCOVA analyses examining the effects of linetype (high runner vs. control), activity (active vs. sedentary), their interaction, and mini-muscle phenotype on food consumption during the first four, last eight, or all 12 weeks of the experiment

Trait	N	Linetype; df = 1,6	Activity; df = 1,6	Act*Ltp; df = 1,6	Mini muscle; df = 1, 70–80
Average food consumption weeks 1–4	99	0.1791	<0.001; A>S	0.0073; CS=HRS<CA<<HRA	0.0990
Average food consumption weeks 5–12	99	0.0983	0.0002; A>S	0.0413; CS<HRS<CA<<HRA	0.2828
Average food consumption weeks 1–12	99	0.1038	0.0001 A>S	0.0186 CS=HRS<CA<<HRA	0.2104

Weekly food consumption was adjusted for mean weekly body mass as explained in the text.

the mice studied here (Copes et al., 2015; Kelly, Gomes, Kolb, Malisch, & Garland, 2017).

Since the publication of the SRH in 1996, the number of mid-Pleistocene hominin species and specimens from previously recognized species has increased substantially (Alemseged et al., 2005, 2006; Berger et al., 2010, 2015; Broadfield et al., 2001; Brown et al., 2004; Cameron, 2003; Carbonell et al., 2008; Finlayson et al., 2006; Haile-Selassie et al., 2015; Leakey et al., 2001, 2012; Lockwood & Tobias, 1999, 2002; Lordkipanidze et al., 2005; Manzi, Mallegni, & Ascenzi, 2001; Morwood et al., 2005; Potts, Behrensmeyer, Deino, Ditchfield, & Clark, 2004; Rightmire, Ponce de León, Lordkipanidze, Margvelashvili, & Zollikofer, 2017; Spoor et al., 2007; Toussaint, Macho, Tobias, Partridge, & Hughes, 2003; Villmoare et al., 2015). CVT values have not typically been included in announcements of these new species, which limits our ability to fill in our knowledge of how CVT has changed among human ancestors (although see Copes & Kimbel, 2016 for an analysis of CVT in fossil hominins). Additional data on CVT for the newly described species may provide more information on the relationships among measures of activity, CVT, and postcranial robusticity metrics. Until then, we suggest rethinking the widely held theory that increased CVT in *H. erectus* was caused by their unique levels of physical activity and circulating growth hormones.

ACKNOWLEDGMENTS

The authors thank Leslie Karpinski, Robert Maciel, Robert Donovan, Rashmi Wijeratne, Nhi Tran, Nohemi LaCombe, Rachael Marsik, Thienanh Nguyen, Wendy Acosta, Nicole Templeton, and Tom Meek for help with the experiments. Experimental design advice was offered by David Green. Steven Tommasini, Svetlana Lublinksy, Heather Jamniczky, and Benedikt Hallgrímson were instrumental in assisting with the microCT scanning and analysis of the skeletal elements. Hormone assays were performed by Laura Hinds and Caren Gundberg. Statistical advice was provided by Rich Feinn. Comments by Bill Kimbel, Gary Schwartz, Mark Spencer, and Matt Ravosa substantially improved earlier versions of this article. The editor, associate editor, an anonymous reviewer, and Campbell Rolian provided comments that greatly improved the manuscript.

ORCID

L. E. Copes http://orcid.org/0000-0002-4337-4016

REFERENCES

Al-Regaiey, K. A., Masternak, M. M., Bonkowski, M., Sun, L., & Bartke, A. (2005). Long-lived growth hormone receptor knockout mice: Interaction of reduced insulin-like growth factor I/insulin signaling and caloric restriction. *Endocrinology*, *146*, 851–860. https://doi.org/10.1210/en.2004-1120

Alemseged, Z., Spoor, F., Kimbel, W. H., Bobe, R., Geraads, D., Reed, D., & Wynn, J. G. (2006). A juvenile early hominin skeleton from Dikika, Ethiopia. *Nature*, *443*, 296–301.

Alemseged, Z., Wynn, J. G., Kimbel, W. H., Reed, D., Geraads, D., & Bobe, R. (2005). A new hominin from the Basal Member of the Hadar Formation, Dikika, Ethiopia and its geological context. *Journal of Human Evolution*, *49*, 499–514.

Andrews, P. J. (1984). An alternative interpretation of the characters used to define *Homo erectus*. *Cour Forsch Inst Senckenberg*, *69*, 167–175.

Antón, S. C. (2002). Evolutionary significance of cranial variation in Asian Homo erectus. *American Journal of Physical Anthropology*, *118*, 301–323.

Antón, S. C. (2003). Natural history of *Homo erectus*. *Yearbook of Physical Anthropology*, *46*, 126–170.

Athreya, S. (2009). A comparative study of frontal bone morphology among Pleistocene hominin fossil groups. *Journal of Human Evolution*, *57*, 786–804. https://doi.org/10.1016/j.jhevol.2009.09.003

Baab, K. L., Freidline, S. E., Wang, S. L., & Hanson, T. (2010). Relationship of cranial robusticity to cranial form, geography and climate in *Homo sapiens*. *American Journal of Physical Anthropology*, *141*, 97–115. https://doi.org/10.1002/ajpa.21120

Baumann, G. (2005). Growth hormone binding proteins. In W. J. Kraemer & A. D. Rogol (Eds.), *The endocrine system in sports and exercise* (pp. 94–109). New York: Blackwell.

Beamer, W. G., Donahue, L. R., & Rosen, C. J. (2000). Insulin-like growth factor I and bone: From mouse to man. *Growth Hormone & IGF Research*, *10 Suppl B()*, S103–S105.

Berger, L. R., de Ruiter, D. J., Churchill, S. E., Schmid, P., Carlson, K. J., Dirks, P. H. G. M., & Kibii, J. M. (2010). *Australopithecus sediba*: A new species of Homo-like australopith from South Africa. *Science*, *328*, 195–204.

Berger, L. R., Hawks, J., de Ruiter, D. J., Churchill, S. E., Schmid, P., Delezene, L. K., … Zipfel, B. (2015). *Homo naledi*, a new species of the genus Homo from the Dinaledi Chamber, South Africa. *eLife*, *4*, https://doi.org/10.7554/eLife.09560

Bernal, V., Perez, S. I., & Gonzalez, P. N. (2006). Variation and causal factors of craniofacial robusticity in Patagonian hunter-gatherers from the Late Holocene. *American Journal of Human Biology*, *18*, 748–765.

Bernstein, R. M., Leigh, S. R., Donovan, S. M., & Monaco, M. H. (2007). Hormones and body size evolution in papionin primates. *American Journal of Physical Anthropology*, *132*, 247–260. https://doi.org/10.1002/ajpa.20521

Bidlingmaier, M., & Freda, P. U. (2010). Measurement of human growth hormone by immunoassays: Current status, unsolved problems and clinical consequences. *Growth Hormone & IGF Research*, *20*, 19–25. https://doi.org/10.1016/j.ghir.2009.09.005

Biewener, A. A. (2005). Biomechanical consequences of scaling. *The Journal of Experimental Biology*, *208*, 1665–1676.

Bilsborough, A., & Wood, B. A. (1988). Cranial morphometry of early hominids: Facial region. *American Journal of Physical Anthropology*, *76*, 61–86.

Bouxsein, M. L., Boyd, S. K., Christiansen, B. A., Guldberg, R. E., Jepsen, K. J., & Muller, R. (2010). Guidelines for assessment of bone microstructure in rodents using micro-computed tomography. *Journal of Bone and Mineral Research*, *25*, 1468–1486. https://doi.org/10.1002/jbmr.141

Broadfield, D. C., Holloway, R. L., Mowbray, K., Silvers, A., Yuan, M. S., & Marquez, S. (2001). Endocast of Sambungmacan 3 (Sm 3): A new *Homo erectus* from Indonesia. *The Anatomical Record*, *262*, 369–379.

Brown, D. A., Johnson, M. S., Armstrong, C. J., Lynch, J. M., Caruso, N. M., Ehlers, L. B., … Moore, R. L. (2007). Short-term treadmill running in the rat: what kind of stressor is it. *J Appl Physiol (1985)*, *103*, 1979–1985. https://doi.org/10.1152/japplphysiol.00706.2007

Brown, P. (1992). Recent human evolution in East Asia and Australasia. *Philosophical Transactions of the Royal Society of London. Series B, Biological Sciences*, *337*, 235–242.

Brown, P. (1994). Cranial vault thickness in Asian *Homo erectus* and *Homo sapiens*. *Cour Forsch Inst Senckenberg*, *171*, 33–46.

Brown, P., Sutikna, T., Morwood, M. J., Soejono, R. P., Jatmiko Saptomo, E. W., & Due, R. A. (2004). A new small-bodied hominin from the Late Pleistocene of Flores, Indonesia. *Nature*, *431*, 1055–1061.

Bruner, E., Písová, H., Martín-Francés, L., Martinón-Torres, M., Arsuaga, J. L., Carbonell, E., & Bermúdez de Castro, J. M. (2017). A human parietal fragment from the late Early Pleistocene Gran Dolina-TD6 cave site, Sierra de Atapuerca, Spain. *C R Paleoevolution*, *16*, 71–81.

Butler, A. A., & Le Roith, D. (2001). Control of growth by the somatropic axis: Growth hormone and the insulin-like growth factors have related and independent roles. *Annual Review of Physiology*, *63*, 141–164. https://doi.org/10.1146/annurev.physiol.63.1.141

Cameron, D. W. (2003). Early hominin speciation at the Plio/Pleistocene transition. *Homo*, *54*, 1–28.

Carbonell, E., Bermúdez de Castro, J. M., Parés, J. M., Pérez-González, A., Cuenca-Bescós, G., Ollé, A., . . . Arsuaga, J. L. (2008). The first hominin of Europe. *Nature*, *452*, 465–469. https://doi.org/10.1038/nature06815

Careau, V., Wolak, M. E., Carter, P. A., & Garland, T. (2013). Limits to behavioral evolution: The quantitative genetics of a complex trait under directional selection. *Evolution*, *67*, 3102–3119. https://doi.org/10.1111/evo.12200

Carlson, K. J., & Byron, C. D. (2008). Building a better organismal model: The role of the mouse. *Integrative and Comparative Biology*, *48*, 321–323.

Carter, P. A., Garland, T., Jr, Dohm, M. R., & Hayes, J. P. (1999). Genetic variation and correlations between genotype and locomotor physiology in outbred laboratory house mice (*Mus domesticus*). *Comparative Biochemistry & Physiology—Part A Molecular & Integrative Physiology*, *123*, 155–162.

Chirchir, H., Kivell, T. L., Ruff, C. B., Hublin, J. J., Carlson, K. J., Zipfel, B., & Richmond, B. G. (2015). Recent origin of low trabecular bone density in modern humans. *Proceedings of the National Academy of Sciencesof the United States of America*, *112*, 366–371. https://doi.org/10.1073/pnas.1411696112

Clemmons, D. R. (2007). Value of insulin-like growth factor system markers in the assessment of growth hormone status. *Endocrinology Metabolism Clinics of North America*, *36*, 109–129. https://doi.org/10.1016/j.ecl.2006.11.008

Conroy, G. C. (2005). *Reconstruction human origins* (2nd ed.). New York: W. W. Norton.

Copes, L. E. (2012). *Comparative and experimental investigations of cranial robusticity in mid-Pleistocene hominins*. PhD, Arizona State University, p. 654.

Copes, L. E., Schutz, H., Dlugosz, E. M., Acosta, W., Chappell, M. A., & Garland, T., Jr. (2015). Effects of voluntary exercise on spontaneous physical activity and food consumption in mice: Results from an artificial selection experiment. *Physiology & Behavior*, *149*, 86–94. https://doi.org/10.1016/j.physbeh.2015.05.025

Copes, L. E., & Kimbel, W. H. (2016). Cranial vault thickness in primates: Homo erectus does not have uniquely thick vault bones. *J Hum Evol*, *90*, 120–134.

Cosman, M. N., Sparrow, L. M., & Rolian, C. (2016). Changes in shape and cross-sectional geometry in the tibia of mice selectively bred for increases in relative bone length. *Journal of Anatomy*, *228*, 940–951. https://doi.org/10.1111/joa.12459

Crevecoeur, I., Brooks, A., Ribot, I., Cornelissen, E., & Semal, P. (2016). Late stone age human remains from Ishango (Democratic Republic of Congo): New insights on Late Pleistocene modern human diversity in Africa. *Journal of Human Evolution*, *96*, 35–57. https://doi.org/10.1016/j.jhevol.2016.04.003

Curnoe, D. (2009). Possible causes and significance of cranial robusticity among Pleistocene-Early Holocene Australians. *Journal of Archaeological Science*, *36*, 980–990.

Curnoe, D., & Green, H. (2013). Vault thickness in two Pleistocene Australian crania. *Journal of Archaeological Science*, *40*, 1310–1318.

Davis, C., Windh, P., & Lauritzen, C. G. (2010). Adaptation of the cranium to spring cranioplasty forces. *Child's Nervous System: Official Journal of the International Society for Pediatric Neurosurgery*, *26*, 367–371. https://doi.org/10.1007/s00381-009-1026-0

Dubois, E. (1937). On the fossil human skulls recently discovered in Java and Pithecanthropus erectus. *Man*, *37*, 1–7.

Eckstein, F., Lochmüller, E.-M., Koller, B., Wehr, U., Weusten, A., Rambeck, W., . . . Wolf, E. (2002). Body composition, bone mass and microstructural analysis in GH-transgenic mice reveals that skeletal changes are specific to bone compartment and gender. *Growth Hormone & IGF Research*, *12*, 116–125.

Eisová, S., Rangel de Lázaro, G., Píšová, H., Pereira-Pedro, S., & Bruner, E. (2016). Parietal bone thickness and vascular diameters in adult modern humans: A survey on cranial remains. *The Anatomical Record*, *299*, 888–896. https://doi.org/10.1002/ar.23348

Felsing, N. E., Brasel, J. A., & Cooper, D. M. (1992). Effect of low and high intensity exercise on circulating growth hormone in men. *The Journal of Clinical Endocrinology and Metabolism*, *75*, 157–162.

Ferguson, V. L., Ayers, R. A., Bateman, T. A., & Simske, S. J. (2003). Bone development and age-related bone loss in male C57BL/6J mice. *Bone*, *33*, 387–398.

Finlayson, C., Giles Pacheco, F., Rodríguez-Vidal, J., Fa, D. A., María Gutierrez López, J., Santiago Pérez, A., . . . Sakamoto, T. (2006). Late survival of Neanderthals at the southernmost extreme of Europe. *Nature*, *443*, 850–853.

Gabriel, S. M., Roncancio, J. R., & Ruiz, N. S. (1992). Growth hormone pulsatility and the endocrine milieu during sexual maturation in male and female rats. *Neuroendocrinology*, *56*, 619–625.

Garland, T., Jr, Morgan, M. T., Swallow, J. G., Rhodes, J. S., Girard, I., Belter, J. G., & Carter, P. A. (2002). Evolution of a small-muscle polymorphism in lines of house mice selected for high activity levels. *Evolution*, *56*, 1267–1275.

Garland, T., Jr, Zhao, M., & Saltzman, W. (2016). Hormones and the evolution of complex traits: Insights from artificial selection on behavior. *Integrative and Comparative Biology*, *56*, 207–224. https://doi.org/10.1093/icb/icw040

Giustina, A., Mazziotti, G., & Canalis, E. (2008). Growth hormone, insulin-like growth factors, and the skeleton. *Endocrine Reviews*, *29*, 535–559. https://doi.org/10.1210/er.2007-0036

Green, D. J., Richmond, B. G., & Miran, S. L. (2012). Mouse shoulder morphology responds to locomotor activity and the kinematic differences of climbing and running. *Journal of Experimental Zoology Part B: Molecular and Developmental Evolution*, *318*, 621–638. https://doi.org/10.1002/jez.b.22466

Haile-Selassie, Y., Gibert, L., Melillo, S. M., Ryan, T. M., Alene, M., Deino, A., . . . Saylor, B. Z. (2015). New species from Ethiopia further expands Middle Pliocene hominin diversity. *Nature*, *521*, 483–488. https://doi.org/10.1038/nature14448

Hallgrímsson, B., Willmore, K., Dorval, C., & Cooper, D. M. (2004). Craniofacial variability and modularity in macaques and mice. *Journal of Experimental Zoology. Part B, Molecular and Developmental Evolution*, *302*, 207–225.

Hoff, J. (2000). Methods of blood collection in the mouse. *Lab Animal*, *29*, 47–53.

Hoyte, D. A. N. (1960). Alizarin as an indicator of bone growth. *Journal of Anatomy*, *94*, 432–442.

Hrdlicka, A. (1910). Contribution to the anthropology of central and Smith Sound Eskimo. *Anthropology Paper of American Museum of Natural Histoty*, *5*, 177–285.

Ionescu, M., & Frohman, L. A. (2006). Pulsatile secretion of growth hormone (GH) persists during continuous stimulation by CJC-1295, a long-acting GH-releasing hormone analog. *Journal of Clinical Endocrinology & Metabolism*, *91*, 4792–4797. https://doi.org/10.1210/jc.2006-1702

Jepsen, K. J. (2011). Functional interactions among morphologic and tissue quality traits define bone quality. *Clinical Orthopaedics and Related Research®*, *469*, 2150–2159. https://doi.org/10.1007/s11999-010-1706-9

Jepsen, K. J., Hu, B., Tommasini, S. M., Courtland, H. W., Price, C., Cordova, M., & Nadeau, J. H. (2009). Phenotypic integration of skeletal traits during growth buffers genetic variants affecting the slenderness of femora in inbred mouse strains. *Mammalian Genome*, *20*, 21–33. https://doi.org/10.1007/s00335-008-9158-1

Jilka, R. L. (2013). The relevance of mouse models for investigating age-related bone loss in humans. *The Journals of Gerontology. Series A, Biological Sciences and Medical Sciences*, *68*, 1209–1217. https://doi.org/10.1093/gerona/glt046

Judex, S., Garman, R., Squire, M., Busa, B., Donahue, L. R., & Rubin, C. (2004). Genetically linked site-specificity of disuse osteoporosis. *Journal of Bone and Mineral Research*, *19*, 607–613. https://doi.org/10.1359/JBMR.040110

Kelly, S. A., Bell, T. A., Selitsky, S. R., Buus, R. J., Hua, K., Weinstock, G. M., … Pomp, D. (2013). A novel intronic single nucleotide polymorphism in the myosin heavy polypeptide 4 gene is responsible for the mini-muscle phenotype characterized by major reduction in hind-limb muscle mass in mice. *Genetics*, *195*, 1385–1395. https://doi.org/10.1534/genetics.113.154476

Kelly, S. A., Czech, P. P., Wight, J. T., Blank, K. M., & Garland, T. (2006). Experimental evolution and phenotypic plasticity of hindlimb bones in high-activity house mice. *Journal of Morphology*, *267*, 360–374. https://doi.org/10.1002/jmor.10407

Kelly, S. A., Gomes, F. R., Kolb, E. M., Malisch, J. L., & Garland, T. Jr, (2017). Effects of activity, genetic selection, and their interaction on muscle metablic capacities and organ masses in mice. *Journal of Experimental Biology*, *220*, 1038–1047.

Lahr, M. M., & Wright, R. V. S. (1996). The question of robusticity and the relationship between cranial size and shape in *Homo sapiens*. *Journal of Human Evolution*, *31*, 157–191.

Lassarre, C., Girad, F., Durand, J., & Raynaud, J. (1974). Kinetics of human growth hormone during submaximal exercise. *Journal of Applied Physiology*, *37*, 826–830.

Leakey, M. G., Spoor, F., Brown, F. H., Gathogo, P. N., Kiarie, C., Leakey, L. N., & McDougall, I. (2001). New hominin genus from eastern Africa shows diverse middle Pliocene lineages. *Nature*, *410*, 433–440.

Leakey, M. G., Spoor, F., Dean, M. C., Feibel, C. S., Anton, S. C., Kiarie, C., & Leakey, L. N. (2012). New fossils from Koobi Fora in northern Kenya confirm taxonomic diversity in early Homo. *Nature*, *488*, 201–204. https://doi.org/10.1038/nature11322

Lieberman, D. E. (1996). How and why humans grow thin skulls: Experimental evidence for systemic cortical robusticity. *American Journal of Physical Anthropology*, *101*, 217–236.

Lieberman, D. E. (2011). *The evolution of the human head*. Cambridge, MA: Belknap Press.

Littell, R. C., Milliken, G. A., Stroup, W. W., Wolfinger, R. D., & Schabenberger, O. (2006). *SAS for mixed models* (2nd ed.). Cary, NC: SAS Publishing.

Lockwood, C. A., & Tobias, P. V. (1999). A large male hominin cranium from Sterkfontein, South Africa, and the status of Australopithecus africanus. *Journal of Human Evolution*, *36*, 637–685.

Lockwood, C. A., & Tobias, P. V. (2002). Morphology and affinities of new hominin cranial remains from Member 4 of the Sterkfontein Formation, Gauteng Province, South Africa. *Journal of Human Evolution*, *42*, 389–450. https://doi.org/10.1006/jhev.2001.0532

Lordkipanidze, D., Vekua, A., Ferring, R., Rightmire, G. P., Agusti, J., Kiladze, G., … Zollikofer, C. P. E. (2005). The earliest toothless hominin skull. *Nature*, *434*, 717–718.

Lublinsky, S., Ozcivici, E., & Judex, S. (2007). An automated algorithm to detect the trabecular-cortical bone interface in micro-computed tomographic images. *Calcified Tissue International*, *81*, 285–293. https://doi.org/10.1007/s00223-007-9063-8

Manzi, G., Mallegni, F., & Ascenzi, A. (2001). A cranium for the earliest Europeans: Phylogenetic position of the hominid from Ceprano, Italy. *Proceedings of the National Academy of Sciences of the United States of America*, *98*, 10011–10016.

Middleton, K. M., Goldstein, B. D., Guduru, P. R., Waters, J. F., Kelly, S. A., Swartz, S. M., & Garland, T. Jr, (2010). Variation in within-bone stiffness measured by nanoindendation in mice bred for high levels of voluntary wheel running. *Journal of Anatomy*, *216*, 121–131.

Morwood, M. J., Brown, P., Jatmiko, Sutikna, T., Saptomo, E. W., Westaway, K. E., … Djubiantono, T. (2005). Further evidence for small-bodied hominins from the Late Pleistocene of Flores, Indonesia. *Nature*, *437*, 1012–1017.

Müller, R., Hahn, M., Vogel, M., Delling, G., & Rüegsegger, P. (1996). Morphometric analysis of noninvasively assessed bone biopsies: Comparison of high-resolution computed tomography and histologic sections. *Bone*, *18*, 215–220. Available at: https://www.ncbi.nlm.nih.gov/pubmed/8703575

Pautke, C., Vogt, S., Tischer, T., Wexel, G., Deppe, H., Milz, S., … Kolk, A. (2005). Polychrome labeling of bone with seven different fluorochromes: Enhancing fluorochrome discrimination by spectral image analysis. *Bone*, *37*, 441–445. https://doi.org/10.1016/j.bone.2005.05.008

Potts, R., Behrensmeyer, A. K., Deino, A. L., Ditchfield, P., & Clark, J. (2004). Small mid-Pleistocene hominin associated with East African Acheulean technology. *Science*, *305*, 75–78.

Price, C., Herman, B. C., Lufkin, T., Goldman, H. M., & Jepsen, K. J. (2005). Genetic variation in bone growth patterns defines adult mouse bone fragility. *Journal of Bone and Mineral Research*, *20*, 1983–1991.

Ramirez-Yañez, G. O., Smid, J. R., Young, W. G., & Waters, M. J. (2005). Influence of growth hormone on the craniofacial complex of transgenic mice. *European Journal of Orthodontics*, *27*, 494–500. https://doi.org/10.1093/ejo/cji028

Rightmire, G. P., Ponce de León, M. S., Lordkipanidze, D., Margvelashvili, A., & Zollikofer, C. P. (2017). Skull 5 from Dmanisi: Descriptive anatomy, comparative studies, and evolutionary significance. *Journal of Human Evolution*, *104*, 50–79. https://doi.org/10.1016/j.jhevol.2017.01.005

Rubin, C. T., & Lanyon, L. E. (1984). Dynamic strain similarity in vertebrates: An alternative to allometric limb bone scaling. *Journal of Theoretical Biology*, *107*, 321–327.

Schilling, A. F., Priemel, M., Timo Beil, F., Haberland, M., Holzmann, T., Catala-Lehnen, P., … Amling, M. (2001). Transgenic and knock out mice in skeletal research: Towards a molecular understanding of the

mammalian skeleton. *Journal of Musculoskeletal & Neuronal Interaction*, *1*, 275–289.

Schutz, H., Jamniczky, H. A., Hallgrímsson, B., & Garland, T. (2014). Shape-shift: Semicircular canal morphology responds to selective breeding for increased locomotor activity. *Evolution*, *68*, 3184–3198. https://doi.org/10.1111/evo.12501

Spoor, F., Leakey, M. G., Gathogo, P. N., Brown, F. H., Antón, S. C., McDougall, I., … Leakey, L. N. (2007). Implications of new early Homo fossils from Ileret, east of Lake Turkana, Kenya. *Nature*, *448*, 688–691. https://doi.org/10.1038/nature05986

Swallow, J. G., Carter, P. A., & Garland, T. (1998). Artificial selection for increased wheel-running behavior in house mice. *Behavior Genetics*, *28*, 227–237.

Swallow, J. G., Garland, T., Jr, Carter, P. A., Zhan, W. Z., & Sieck, G. C. (1998). Effects of voluntary activity and genetic selection on aerobic capacity in house mice (*Mus domesticus*). *Journal of Applied Physiology*, *84*, 69–76.

Swallow, J. G., Koteja, P., Carter, P. A., & Garland, T. (2001). Food consumption and body composition in mice selected for high wheel-running activity. *Journal of Comparative Physiology. B, Biochemical, Systemic, and Environmental Physiology*, *171*, 651–659.

Tommasini, S. M., Nasser, P., Hu, B., & Jepsen, K. J. (2007). Biological co-adaptation of morphological and composition traits contributes to mechanical functionality and skeletal fragility. *Journal of Bone and Mineral Research*, *23*, 236–246. https://doi.org/10.1359/jbmr.071014

Tommasini, S. M., Wearne, S. L., Hof, P. R., & Jepsen, K. J. (2008). Percolation theory relates corticocancellous architecture to mechanical function in vertebrae of inbred mouse strains. *Bone*, *42*, 743–750. https://doi.org/10.1016/j.bone.2007.12.009

Toussaint, M., Macho, G. A., Tobias, P. V., Partridge, T. C., & Hughes, A. R. (2003). The third partial skeleton of a late Pliocene hominin (Stw 431) from Sterkfontein, South Africa. *South African Journal of Science*, *99*, 215–223.

Tryon, C. A., Crevecoeur, I., Faith, J. T., Ekshtain, R., Nivens, J., Patterson, D., … Spoor, F. (2015). Late Pleistocene age and archaeological context for the hominin calvaria from GvJm-22 (Lukenya Hill, Kenya). *Proceedings of the National Academy of Sciences of the United States of America*, *112*, 2682–2687. https://doi.org/10.1073/pnas.1417909112

van der Meulen, M. C., Jepsen, K. J., & Mikic, B. (2001). Understanding bone strength: Size isn't everything. *Bone*, *29*, 101–104.

van Ingen Schenau, G. J. (1980). Some fundamental aspects of the biomechanics of overground versus treadmill locomotion. *Med Sci Sports Exerc*, *12*, 257–261.

Villmoare, B., Kimbel, W. H., Seyoum, C., Campisano, C. J., DiMaggio, E. N., Rowan, J., … Reed, K. E. (2015). Early Homo at 2.8 Ma from Ledi-Geraru, Afar, Ethiopia. *Science (New York, N.Y.)*, *347*, 1352–1355. https://doi.org/10.1126/science.aaa1343

Wallace, I. J., & Garland, T. (2016). Mobility as an emergent property of biological organization: Insights from experimental evolution. *Evolutionary Anthropology: Issues, News, and Reviews*, *25*, 98–104. https://doi.org/10.1002/evan.21481

Wallace, I. J., Garland, T., Jr, Wallace, S. A., Middleton, K. M., Kelly, S. A., Judex, S., & Demes, B. (2011). Genetic and epigenetic effects on diaphyseal morphology in selectively bred mice with the mini-muscle allele (abstract). *Integrative & Comparative Biology*, *51*, E263.

Wallace, I. J., Tommasini, S. M., Judex, S., Garland, T., Jr., & Demes, B. (2012). Genetic variations and physical activity as determinants of limb bone morphology: An experimental approach using a mouse model. *American Journal of Physical Anthropology*, *148*, 24–35. https://doi.org/10.1002/ajpa.22028

Weidenreich, F. (1943). *The skull of Sinanthropus pekinensis: A comparative study on a primitive hominid skull*. Geological Survey of China.

Wolpoff, M. H. (1999). *Paleoanthropology*. New York: McGraw-Hill.

Yang, L., Zhang, P., Liu, S., Samala, P. R., Su, M., & Yokota, H. (2007). Measurement of strain distributions in mouse femora with 3D-digital speckle pattern interferometry. *Optics & Lasers in Engineering*, *45*, 843–851. https://doi.org/10.1016/j.optlaseng.2007.02.004

Yanagita, S., Amemiya, S., Suzuki, S., & Kita, I. (2007). Effects of spontaneous and forced running on activation of hypothalamic corticotropin-releasing hormone neurons in rats. *Life Sci*, *80*, 356–363. doi: 10.1016/j.lfs.2006.09.027

Young, N. M., Hallgrimsson, B., & Garland, T. Jr, (2009). Epigenetic effects of integration of limb bone lengths in a mouse model: Selective breeding for high voluntary locomotor activity. *Journal of Evolutionary Biology*, *36*, 88–99.

Young, W. G., Ramirez-Yanez, G. O., Daley, T. J., Smid, J. R., Coshigano, K. T., Kopchick, J. J., & Waters, M. J. (2004). Growth hormone and epidermal growth factor in salivary glands of giant and dwarf transgenic mice. *Journal of Histochemistry & Cytochemistry*, *52*, 1191–1197. https://doi.org/10.1369/jhc.4A6294.2004

SUPPORTING INFORMATION

Additional Supporting Information may be found online in the supporting information tab for this article.

How to cite this article: Copes LE, Schutz H, Dlugsoz EM, Judex S, Garland T Jr. Locomotor activity, growth hormones, and systemic robusticity: An investigation of cranial vault thickness in mouse lines bred for high endurance running. *Am J Phys Anthropol*. 2018;166:442–458. https://doi.org/10.1002/ajpa.23446

				Linetype			Activity			Activity * Linetype			Mini		
Week	Model	Original n	n after outliers removed	df	p	parameter estimate	df	p	parameter estimate	df	p	parameter estimate	df	p	parameter estimate
	wk1run4	50		6	0.0005	-3681.61	-	-	-	-	-	-	41	0.1811	-943.5000
	wk1int4	50		6	0.011	-113.07	-	-	-	-	-	-	41	0.1067	-62.5049
	wk1max4	50		6	0.0071	-15.8043	-	-	-	-	-	-	41	0.556	-2.2793
	wk1rpm4	50		6	0.0038	-9.3499	-	-	-	-	-	-	41	0.6118	-1.1520
	wk1htot4	99		6	0.088	4.6392	6	0.0001	113.09	6	0.0217	-58.4933	82	0.4093	12.7125
1	wk1htot4		98	6	0.1291	13.6224	6	<0.0001	119.79	6	0.0138	-65.2322	81	0.6016	7.2416
	wk1hmx4	99		6	0.557	0.02124	6	0.0003	0.1234	6	0.0397	-0.06518	82	0.5169	0.0182
	wk1hmx4		97	6	0.8561	0.03786	6	0.0003	0.1236	6	0.0098	-0.08225	80	0.337	0.0199
	wk1hint4	99		6	0.0888	-35.9202	6	0.0128	82.192	6	0.4984	-28.0432	82	0.8096	7.5366
	wk1hint4		98	6	0.1662	-15.9328	6	0.0094	96.0888	6	0.3356	-41.8305	81	0.8019	-7.4172
	wk1hapm4	99		6	0.5137	0.03764	6	0.0001	0.1774	6	0.0158	-0.09845	82	0.2187	0.0262
	wk2run5	50		6	0.0024	-7303.67	-	-	-	-	-	-	41	0.383	-1469.0100
	wk2int5	50		6	0.0396	-85.1119	-	-	-	-	-	-	41	0.1555	-61.2003
	wk2max5	50		6	0.0057	-24.8016	-	-	-	-	-	-	41	0.9124	-0.5136
	wk2rpm5	50		6	0.0055	-16.889	-	-	-	-	-	-	41	0.9146	0.3459
2	wk2htot3	99		6	0.7369	23.8467	6	<0.0001	102.89	6	0.0145	-54.0561	82	0.8703	1.9184
	wk2hmx3	99		6	0.8669	0.02556	6	0.0017	0.08319	6	0.0348	-0.05602	82	0.2902	0.0186
	wk2hmx3		98	6	0.9153	0.03282	6	0.002	0.08305	6	0.0188	-0.06296	81	0.2348	0.0184
	wk2hint3	99		6	0.514	74.1932	6	0.0283	125.82	6	0.0672	-109.96	82	0.3365	-33.3632
	wk2hapm3	99		6	0.5156	0.01089	6	<0.0001	0.1297	6	0.1005	-0.04294	82	0.221	0.0235

	wk3run5	50		6	0.017	-9223.21	-	-	-	-	-	-	41	0.5848	-1237.6400
	wk3int5	50		6	0.0272	-125.9	-	-	-	-	-	-	41	0.5609	-29.5476
	wk3max5	50		6	0.0107	-25.8172	-	-	-	-	-	-	41	0.7664	1.4478
	wk3rpm5	50		6	0.0148	-17.4028	-	-	-	-	-	-	41	0.8068	-0.9716
3	wk3htot5	99		6	0.8853	32.3405	6	<0.0001	119.13	6	0.005	-61.9025	82	0.3103	11.9211
	wk3hmx5	99		6	0.6362	0.03471	6	0.0003	0.1066	6	0.0499	-0.06268	82	0.3851	0.0176
	wk3hint5	99		6	0.3998	97.6421	6	0.0097	161.22	6	0.0213	-146	82	0.6428	-15.3356
	wk3hapm5	99		6	0.8873	0.02574	6	0.0001	0.1476	6	0.1572	-0.04569	82	0.2568	0.0248
	wk4run5	50		6	0.0061	-10805	-	-	-	-	-	-	41	0.5436	-1450.0300
	wk4int5	50		6	0.0055	-149.26	-	-	-	-	-	-	41	0.943	-3.1705
	wk4max5	50		6	0.0058	-26.3459	-	-	-	-	-	-	41	0.8538	-0.9354
	wk4max5		49	6	0.0046	-27.4285	-	-	-	-	-	-	40	0.889	-0.6347
	wk4rpm5	50		6	0.0088	-18.6684	-	-	-	-	-	-	41	0.6199	-2.0424
	wk4rpm5		49	6	0.0084	-20.8361	-	-	-	-	-	-	40	0.6113	2.0041
4	wk4htot5	100		6	0.7097	13.0972	6	0.0004	105.1	6	0.1714	-37.1527	83	0.9811	-0.3890
	wk4htot5		98	6	0.2265	8.5026	6	<0.0001	108.89	6	0.0413	-41.6194	81	0.2453	13.5966
	wk4hmx5	100		6	0.3137	0.02875	6	0.0475	0.05659	6	0.9545	-0.00265	83	0.2499	-0.0365
	wk4hmx5		99	6	0.7893	0.01438	6	0.0003	0.09239	6	0.1014	-0.03754	82	0.8547	0.0033
	wk4hint5	100		6	0.8378	0.2283	6	0.0086	87.2816	6	0.751	-13.9071	83	0.736	-11.4817
	wk4hint5		99	6	0.2996	-7.3288	6	0.0042	111	6	0.3916	-38.0126	82	0.675	12.2579
	wk4hapm5	100		6	0.8018	0.02591	6	0.001	0.1437	6	0.3715	-0.04002	83	0.6811	-0.0101
	wk4hapm5		99	6	0.573	0.01642	6	0.0002	0.1563	6	0.1368	-0.05342	82	0.3823	0.0180
	wk5run6	50		6	0.0076	-9489.34	-	-	-	-	-	-	41	0.1838	-2928.1500
	wk5run6		49	6	0.0094	-10909	-	-	-	-	-	-	40	0.8896	-278.7900
5	wk5int6	50		6	0.0068	-147.41	-	-	-	-	-	-	41	0.7178	-16.4039
	wk5max6	50		6	0.0057	-24.026	-	-	-	-	-	-	41	0.4182	-4.1599
	wk5max6		49	6	0.0058	-27.558	-	-	-	-	-	-	40	0.5625	2.7180

	wk5rpm6	50		6	0.0088	-16.9678	-	-	-		-	-	-		41	0.2753	-4.3690
	wk5rpm6		49	6	0.0086	-19.5281	-	-	-		-	-	-		40	0.905	0.4358
	wk5htot5	99		6	0.3009	9.0176	6	0.0001		104.15	6	0.065		-41.5891	82	0.1099	21.2285
	wk5hmx5	99		6	0.942	0.0185	6	0.0003		0.09762	6	0.0996		-0.03984	82	0.5494	0.0127
	wk5hint5	99		6	0.2101	-7.3332	6	0.0326		89.6656	6	0.2606		-55.5751	82	0.9113	3.4205
	wk5hint5		98	6	0.1344	-7.33	6	0.0394		89.6683	6	0.1632		-67.6302	81	0.9065	3.4130
	wk5hapm5	99		6	0.8464	0.02358	6	<0.0001		0.1536	6	0.1896		-0.04086	82	0.1	0.0325
	wk6run5	48		6	0.0017	-10308	-	-	-		-	-	-		39	0.2357	-2595.4500
	wk6int5	48		6	0.0051	-156.98	-	-	-		-	-	-		39	0.8131	45.6239
	wk6max5	48		6	0.0056	-24.5652	-	-	-		-	-	-		39	0.3742	-4.8294
	wk6max5		47	6	0.0052	-27.9811	-	-	-		-	-	-		38	0.7385	1.6815
	wk6rpm5	48		6	0.0051	-17.6917	-	-	-		-	-	-		39	0.3329	-4.0683
	wk6rpm5		47	6	0.005	-20.0958	-	-	-		-	-	-		38	0.9352	0.3289
6	wk6htot5	99		6	0.1713	5.0613	6	<0.0001		110.79	6	0.0429		-47.7231	82	0.417	12.4565
	wk6htot5		97	6	0.3781	11.1235	6	<0.0001		109.57	6	0.0311		-45.9651	80	0.4467	11.5842
	wk6hmx5	99		6	0.841	0.01428	6	0.0003		0.1068	6	0.1836		-0.03649	82	0.4532	0.0171
	wk6hmx5		96	6	0.6503	0.03257	6	0.0002		0.09816	6	0.0454		-0.04626	79	0.9798	-0.0005
	wk6hint5	99		6	0.1573	-12.3009	6	0.0163		93.1973	6	0.2179		-54.82	82	0.6486	-14.2422
	wk6hapm5	99		6	0.7359	0.01703	6	<0.0001		0.1572	6	0.12756		-0.04561	82	0.1608	0.0313
	wk6hapm5		97	6	0.9911	0.02292	6	<0.0001		0.1568	6	0.1072		-0.04542	80	0.5063	0.0146
	wk7run6	50		6	0.0018	-8709.79	-	-	-		-	-	-		41	0.1164	-3097.9500
	wk7run6		49	6	0.0016	-7803.15	-	-	-		-	-	-		40	0.0168	-4309.6000
	wk7int6	50		6	0.0034	-136.53	-	-	-		-	-	-		41	0.6647	-16.5973
7	wk7max6	50		6	0.01	-21.4781	-	-	-		-	-	-		41	0.2578	-6.0247
	wk7max6		49	6	0.0078	-24.0828	-	-	-		-	-	-		40	0.7909	-1.3551
	wk7rpm6	50		6	0.0083	-14.7595	-	-	-		-	-	-		41	0.1721	-5.3046
	wk7rpm6		49	6	0.0069	-16.8314	-	-	-		-	-	-		40	0.6286	-1.7859

	wk7htot6	99		6	0.0201	-6.8275	6	<0.0001	136.67	6	0.0171	-68.8191	82	0.0821	29.4409
	wk7htot6		98	6	0.0572	-2.7501	6	<0.0001	122.82	6	0.0176	-54.2416	81	0.27	17.0261
	wk7hmx6	99		6	0.4943	-0.00094	6	0.0006	0.09536	6	0.2765	-0.0294	82	0.4961	0.0158
	wk7hmx6		98	6	0.6363	0.006767	6	0.0008	0.09509	6	0.194	-0.0397	81	0.5575	0.0135
	wk7hint6	99		6	0.0674	-36.3004	6	0.0018	130.86	6	0.2253	-53.1035	82	0.6074	17.8914
	wk7hapm6	99		6	0.0734	0.002082	6	<0.0001	0.1745	6	0.038	-0.07154	82	0.0512	0.0393
	wk7hapm6		98	6	0.2653	0.006673	6	<0.0001	0.1589	6	0.0584	-0.05433	81	0.2122	0.0249
	wk8run6	51		6	0.0028	-7613.67	-	-	-	-	-	-	42	0.3381	-1818.5900
	wk8int6	51		6	0.0292	-120.67	-	-	-	-	-	-	42	0.9428	3.7646
	wk8int6		50	6	0.0241	-108.52	-	-	-	-	-	-	41	0.9363	3.6346
	wk8max6	51		6	0.0067	-21.2463	-	-	-	-	-	-	42	0.3276	-5.4505
	wk8rpm6	51		6	0.0069	-14.0553	-	-	-	-	-	-	42	0.2574	-4.3875
	wk8rpm6		50	6	0.0063	-16.1288	-	-	-	-	-	-	41	0.785	-1.0416
8	wk8htot6	99		6	0.0114	-16.9145	6	0.0002	117.82	6	0.0271	-60.8111	82	0.2139	20.9504
	wk8htot6		98	6	0.0334	-12.2207	6	<0.0001	103.79	6	0.0389	-46.0533	81	0.6579	6.8168
	wk8hmx6	99		6	0.2252	-0.04021	6	0.0008	0.0613	6	0.5151	0.01524	82	0.5489	0.0151
	wk8hmx6		98	6	0.2596	-0.03212	6	0.0008	0.0613	6	0.721	0.00778	81	0.5234	0.0151
	wk8hint6	99		6	0.0863	-39.7212	6	0.0266	100.87	6	0.4365	-44.7998	82	0.9713	1.3524
	wk8hapm6	99		6	0.0244	-0.01814	6	0.0001	0.1515	6	0.0842	-0.05778	82	0.1062	0.0322
	wk8hapm6		98	6	0.0496	-0.01411	6	<0.0001	0.1366	6	0.138	-0.04216	81	0.2474	0.0203
	wk9run6	49		6	0.0079	-8127.94	-	-	-	-	-	-	40	0.2193	-2749.8500
	wk9run6		48	6	0.0087	-9489.33	-	-	-	-	-	-	39	0.8779	-336.9200
	wk9int6	49		6	0.061	-103.92	-	-	-	-	-	-	40	0.7001	-21.2282
9	wk9int6		48	6	0.0186	-117.19	-	-	-	-	-	-	39	0.6031	-23.8880
	wk9max6	49		6	0.0127	-22.3161	-	-	-	-	-	-	40	0.2937	-6.0592
	wk9max6		48	6	0.0102	-25.3975	-	-	-	-	-	-	39	0.9485	-0.3549
	wk9rpm6	49		6	0.0138	-14.6488	-	-	-	-	-	-	40	0.1893	-5.5307

	wk9rpm6		48	6	0.0099	-16.9895	-	-	-		-	-	-	39	0.7074	-1.4761
	wk9htot6	100		6	0.111	-1.6967	6	0.0005		109.97	6	0.0969	-49.2987	83	0.4408	13.9377
	wk9htot6		97	6	0.1862	5.6585	6	<0.0001		111.01	6	0.0384	-49.7215	80	0.5751	-8.3924
	wk9hmx6	100		6	0.4703	-0.03142	6	0.0179		0.05851	6	0.5953	0.0259	83	0.0742	0.0580
	wk9hmx6		98	6	0.996	0.0115	6	0.0064		0.08787	6	0.5559	-0.02324	81	0.6426	-0.0109
	wk9hint6	100		6	0.9112	8.582	6	0.081		75.0588	6	0.6907	-24.9516	83	0.6764	-17.7059
	wk9hint6		97	6	0.836	35.5916	6	0.0167		118.08	6	0.11	-85.7914	80	0.2312	-46.3374
	wk9hapm6	100		6	0.0202	-0.01596	6	<0.0001		0.1584	6	0.0622	-0.05789	83	0.0094	0.0496
	wk9hapm6		98	6	0.0224	-0.00618	6	<0.0001		0.1577	6	0.0211	-0.05683	81	0.1336	0.0222
	wk10run5	49		6	0.0062	-6813.96	-	-	-		-	-	-	40	0.2311	-2298.7200
	wk10int5	49		6	0.0305	-94.5822	-	-	-		-	-	-	40	0.7123	-15.7858
	wk10max5	49		6	0.011	-19.6951	-	-	-		-	-	-	40	0.285	-5.7637
	wk10rpm5	49		6	0.0144	-13.3847	-	-	-		-	-	-	40	0.2487	-4.8174
	wk10rpm5		48	6	0.0112	-15.4536	-	-	-		-	-	-	39	0.7395	-1.3593
	wk10hto5	98		6	0.012	-13.9443	6	0.0001		122.83	6	0.0178	-64.9721	81	0.0463	33.2140
10	wk10hto5		96	6	0.0153	-7.278	6	<0.0001		121.43	6	0.0072	-63.5155	79	0.305	14.6981
	wk10hmx5	98		6	0.4228	-0.0348	6	0.0465		0.0406	6	0.6031	0.02282	81	0.0427	0.0703
	wk10hmx5		97	6	0.02603	-0.01589	6	0.0016		0.07732	6	0.6274	-0.01324	80	0.4241	0.0159
	wk10hit5	98		6	0.1102	-13.8681	6	0.0055		135.21	6	0.1164	-81.8458	81	0.4345	28.7526
	wk10hit5		97	6	0.0834	-1.6091	6	0.0032		158.85	6	0.0559	-105.57	80	0.8564	-5.9041
	wk10ham5	98		6	0.0343	-0.02005	6	0.0002		0.149	6	0.1257	-0.05468	81	0.0095	0.0586
	wk10ham5		96	6	0.0306	-0.01144	6	<0.0001		0.1527	6	0.0449	-0.05844	79	0.0676	0.0343
	wk11run6	49		6	0.019	-4088.94	-	-	-		-	-	-	40	0.1613	-2290.3100
	wk11run6		48	6	0.0528	-3317.91	-	-	-		-	-	-	39	0.0501	-3274.6600
11	wk11int6	49		6	0.0077	-110.13	-	-	-		-	-	-	40	0.9485	-2.3337
	wk11int6		48	6	0.0452	-96.4727	-	-	-		-	-	-	39	0.9426	-2.9826
	wk11max6	49		6	0.0792	-10.4199	-	-	-		-	-	-	40	0.1976	-8.1345

	wk11rpm6	49		6	0.0453	-7.5257	-	-	-		-	-	-	40	0.1521	-5.3825
	wk11hto6	98		6	0.2931	3.9725	6	0.0005		102.76	6	0.0887		-47.9353	81	0.7226	7.0977
	wk11hto6		95	6	0.5665	10.4933	6	<0.0001		93.3826	6	0.0495		-38.4036	78	0.4833	-11.3759
	wk11hmx6	98		6	0.8886	-0.01424	6	0.0235		0.05395	6	0.6418		0.0209	81	0.0712	0.0605
	wk11hmx6		97	6	0.9082	0.005599	6	0.0005		0.09077	6	0.5615		-0.01527	80	0.8626	0.0035
	wk11hit6	98		6	0.2432	-12.3157	6	0.0219		90.1017	6	0.2914		-49.3027	81	0.5262	22.6998
	wk11hit6		97	6	0.2382	-0.5387	6	0.0054		112.87	6	0.0929		-72.1277	80	0.771	-9.8329
	wk11ham6	98		6	0.5806	0.01095	6	0.0003		0.1421	6	0.1883		-0.04769	81	0.4115	0.0211
	wk11ham6		96	6	0.6491	0.01696	6	<0.0001		0.1458	6	0.0527		-0.05168	79	0.8664	0.0036
	wk12run4	49		6	0.0095	-4758.43	-	-	-		-	-	-	40	0.1771	-2244.2300
	wk12int4	49		6	0.0461	-112.94	-	-	-		-	-	-	40	0.8527	-10.1869
	wk12int4		48	6	0.1189	-105.38	-	-	-		-	-	-	39	0.8068	14.1780
	wk12max4	49		6	0.0564	-10.8407	-	-	-		-	-	-	40	0.2434	-6.9785
	wk12rpm4	49		6	0.0228	-8.2882	-	-	-		-	-	-	40	0.2034	-4.4978
	wk12hto4	98		6	0.0609	-11.3941	6	0.0021		124.71	6	0.1053		-67.3157	81	0.0782	41.0569
12	wk12hto4		97	6	0.0372	-9.7862	6	0.0004		109.66	6	0.071		-52.1882	80	0.0365	35.7318
	wk12hmx4	98		6	0.6279	-0.01262	6	0.0115		0.08371	6	0.9744		0.00154	81	0.1201	0.0532
	wk12hmx4		97	6	0.4614	0.00617	6	0.0003		0.1218	6	0.1903		-0.03981	80	0.9824	0.0005
	wk12hit4	98		6	0.1187	-31.7036	6	0.1035		70.0006	6	0.4434		-41.9289	81	0.1378	55.5035
	wk12hit4		97	6	0.0974	-21.1691	6	0.0372		81.838	6	0.2049		-63.8659	80	0.4589	25.9218
	wk12ham4	98		6	0.08	-0.01073	6	0.0005		0.1859	6	0.1166		-0.07886	81	0.0354	0.0599
	wk12ham4		96	6	0.0356	-0.00431	6	<0.0001		0.186	6	0.0316		-0.07947	79	0.0527	0.0407